

Removal of ethylbenzene and n-hexane from air streams by adsorption processes with Activated Carbon

by

Alfarouk Abbas Alio Serki

Final dissertation submitted to

Escola Superior de Tecnologia e Gestão

Instituto Politécnico de Bragança

In agreement with

Université Libre de Tunis

to the fulfilment of the requirements for the Master of Science Degree in

Chemical Engineering

This work was carried out under the guidance of

Prof. Doctor José António Correia Silva

And co-supervised by

Doctor Khalil Zaghdoudi

Academic Year

2020-2021

ACKNOWLEDGMENTS

First and foremost, praise and thanks to the almighty Allah for giving me the ability to understand the workload and the courage to do it. I dedicate this work to my dear mother Mariama Maidagi in particular and globally to my family and to those who are no longer there.

Then, I would like to express my deep gratitude to my supervisor at the IPB Prof. Dr. José António Correia Silva for giving me the chance to work on this subject, for his support, advice, and guidance. My thanks go to Dr. Khalil Zaghoudi my supervisor at the ULT for his contributions.

I would also like to thank Luca Zafanelli for his listening and his help at all times. My work certainly would not have been the same.

My thanks also go to Adriano Henrique for his help in my early days in the laboratory and his punctual contributions.

My thanks also go to my friends and colleagues who have supported and encouraged me throughout this period of work.

ABSTRACT

The development of chemical engineering process technologies in recent years has led to an increase in the quantities of volatile organic compounds (VOCs) released into the atmosphere. Some of these VOCs such as ethylbenzene and n-hexane, in addition to being polluting, are found to be harmful to human health. Multiple techniques have been developed for the capture of these VOCs in ambient air. Adsorption processes are recognized as being very competitive for the removal of VOCs regarding the efficiency and the costs of its application.

In this work, the adsorption equilibria of ethylbenzene and n-hexane in a commercial activated carbon (Norit RB4) was studied at the temperatures of 398 K, 423 K and 448 K and pressures between 0.01 up to 0.1 bar using gas chromatography. At the temperature of 398 K and partial pressure of 0.1 bar the sorption uptake capacity of ethylbenzene is around 2.34 mol.kg^{-1} , with a heat of adsorption in the range of $50.0 \sim 59.5 \text{ kJ.mol}^{-1}$. For similar conditions the n-hexane sorption uptake is smaller being around 1.61 mol.kg^{-1} with a heat of adsorption in the range of $52.5 \sim 59.2 \text{ kJ.mol}^{-1}$. The experimental adsorption equilibrium data was modelled with the Langmuir, Freundlich, Sips, Toth and Redlich-Peterson adsorption isotherms. It is shown that the best isotherm model that fits the experimental data is given by the Toth isotherm for the ethylbenzene, while the Freundlich isotherm is best suited for n-hexane.

RÉSUMÉ

Le développement des technologies de procédés de génie chimique au cours des dernières années a entraîné une augmentation des quantités de composés organiques volatils (COV) libérées dans l'atmosphère. Certains de ces COV tels que l'éthylbenzène et le n-hexane, en plus d'être polluants, se révèlent nocifs pour la santé humaine. De multiples techniques ont été développées pour la capture de ces COV dans l'air ambiant. Les procédés d'adsorption sont reconnus comme étant très compétitifs pour l'élimination des COV en ce qui concerne l'efficacité et les coûts de leur application.

Dans ce travail, les équilibres d'adsorption de l'éthylbenzène et du n-hexane dans un charbon actif commercial (Norit RB4) ont été étudiés à des températures de 398 K, 423 K et 448 K et à des pressions allant jusqu'à 0,1 bar à l'aide d'une technique de chromatographie en phase gazeuse. À la température de 398 K et à la pression partielle de 0,1 bar, la capacité d'adsorption d'adsorption de l'éthylbenzène est d'environ $2,34 \text{ mol.kg}^{-1}$, avec une chaleur isostérique d'adsorption comprise entre 50,0 et 59,5 kJ.mol^{-1} . Pour des conditions similaires, l'adsorption de la sorption du n-hexane est plus faible étant d'environ $1,61 \text{ mol.kg}^{-1}$ avec une chaleur isostérique comprise entre 52,5 et 59,2 kJ.mol^{-1} . Les données expérimentales d'équilibre d'adsorption ont été modélisées avec les isothermes d'adsorption de Langmuir, Freundlich, Sips, Toth et Redlich-Peterson. Il est démontré que le meilleur modèle isotherme qui correspond aux données expérimentales est donné par l'isotherme de Toth pour l'éthylbenzène, tandis que l'isotherme de Freundlich est la mieux adaptée au n-hexane.

RESUMO

O desenvolvimento de tecnologias de engenharia química nos últimos anos levou a um aumento da quantidade de compostos orgânicos voláteis (COV) libertados para a atmosfera. Alguns destes COV, como o etilbenzeno e o n-hexano, além de poluir, são prejudiciais à saúde humana. Foram desenvolvidas múltiplas técnicas para a captura destes COV no ar ambiente. Os processos de adsorção são reconhecidos como altamente competitivos para a remoção do VOC em termos de eficiência e custos da sua aplicação.

Neste trabalho, foram estudados os equilíbrios de etilbenzeno e n-hexano num carbono ativado comercial (Norit RB4) a temperaturas de 398 K, 423 K e 448 K e a pressões até 0,1 bar utilizando uma técnica de cromatografia gasosa. À temperatura de 398 K e à pressão parcial de 0,1 bar, a capacidade de absorção de etilbenzeno é de cerca de $2,34 \text{ mol.kg}^{-1}$ com um calor isotérico de adsorção entre 50,0 e 59,5 kJ.mol^{-1} . Para condições semelhantes, a absorção de sorption n-hexano é menor sendo cerca de $1,61 \text{ mol.kg}^{-1}$ com calor isotérico entre 52,5 e 59,2 kJ.mol^{-1} . Os dados experimentais do equilíbrio de adsorção foram modelados com isotérmicos de adsorção de Langmuir, Freundlich, Sips, Toth e Redlich-Peterson. Mostra-se que o melhor modelo isotérmico que corresponde aos dados experimentais é dado pelo isotérmico toth para etilbenzeno, enquanto o isotérmico freundlich é mais adequado para n-hexano.

LIST OF CONTENT

ABSTRACT.....	ii
LIST OF FIGURES	vii
LIST OF TABLES	viii
NOMENCLATURE	ix
INTRODUCTION	1
1. STATE OF THE ART.....	4
1.1 Harmfulness of volatile organic compounds.....	4
1.2 Adsorption.....	5
1.3 Physical adsorption and chemisorption.....	6
1.3.1 Mobile and Immobile Adsorption.....	7
1.3.2 Monolayer and Multilayer Adsorption and Capillary Condensation.....	7
1.4 Adsorbents.....	8
1.5 Activated carbon	11
1.6 Adsorption isotherms	13
1.6.1 Type I isotherm.....	14
1.6.2 Type II isotherm.....	14
1.6.3 Type III isotherm	15
1.6.4 Type IV and V isotherms.....	15
1.6.5 Type VI isotherm	15
2. EXPERIMENTAL SECTION.....	16
2.1 Measurement of gas adsorption isotherms in a fixed bed by chromatography	16
2.1.1 Chromatographic technique	16
2.1.2 Breakthrough Curves	17

2.2	Adsorption Equilibrium Isotherm models.....	17
2.2.1	Langmuir model.....	17
2.2.2	Freundlich model	18
2.2.3	Sips model.....	19
2.2.4	Toth model	20
2.2.5	Redlich-Peterson model	21
2.3	The Isotheric heat of adsorption	21
2.4	Experimental Apparatus for Measuring Breakthrough Curves.....	22
2.5	Materials and operating conditions	25
2.6	Experimental procedure	28
3.	RESULTS AND DISCUSSION.....	29
3.1	Breakthrough curves	29
3.2	Modelling of adsorption equilibrium isotherms.....	32
3.2.1	Ethylbenzene isotherm model fitting	33
3.2.2	n-hexane isotherm mode fitting	35
	CONCLUSIONS.....	37
	REFERENCES	38

LIST OF FIGURES

Figure 1 Classification of different VOCs	1
Figure 2 VOCs emission from different sources in China in 2015	2
Figure 3 Classification of VOCs degradation methods	3
Figure 4 The shape of the five type of adsorption isotherms according to the IUPAC	14
Figure 5 Schematic representation of the fixed bed adsorption and the corresponding observed breakthrough curve.....	16
Figure 6 Representation of the integrated area in the breakthrough curve for the calculation of the sorption uptake in a single component experiment.....	17
Figure 7 Schematic diagram of the adsorption equilibrium apparatus used to measure adsorption equilibrium data through breakthrough curves: (MFC) mass flow controller; (SP) syringe pump; (AC) adsorption column; (EC) expansion column; (EPC) electronic pressure control; (TCD) thermal conduct detector; (V1) and (V3) 3-way ball valve;(V2) flow metering valve;(BF) bubble flowmeter, and (①②③④) streams.	24
Figure 8 Real view of the chromatographic adsorption equilibrium apparatus: a) detailed view of the overall system, and b) close-up of the inside the chromatograph oven.	24
Figure 9 Adsorption/Desorption H ₂ isotherm at 77.35 K on activated carbon Norit RB 4 sample for its textural characterization.	26
Figure 10 SEM micrographs of the Norit RB 4 activated carbon: Magnified: A)x17, B)x500, C)x2000, D)x4000, E)x5000 and F)x10000	27
Figure 11 Experimental breakthrough curves of ethylbenzene in activated carbon Norit RB4 at (a) 398, (b) 423, and (c) 448 K and partial pressure up to 0.1 bar. Experimental conditions are given in Table 5.	29
Figure 12 Experimental breakthrough curves of n-hexane in activated carbon Norit RB4 at (a) 398, (b) 423, and (c) 448 K and partial pressure up to 0.1 bar. Experimental conditions are given in Table 5.	30
Figure 13 Experimental adsorption equilibrium isotherms of a) ethylbenzene and b) n-hexane on NORIT RB 4 Activated carbon.....	32

Figure 14 Experimental adsorption equilibrium of ethylbenzene onto Activated carbon Norit RB4 at 398, 423, and 448 K and partial pressure up to 0.1 bar and isotherm models fitting comparison.	33
Figure 15 Parity plot of fitted Toth isotherm model for adsorption of ethylbenzene on NORIT RB 4 activated carbon.	34
Figure 16 Experimental adsorption equilibrium of n-hexane onto Activated carbon Norit RB4 at 398, 423, and 448 K and partial pressure up to 0.1 bar and isotherm models (a) Toth, (b) Sips, (c) Redlich-Peterson, (d) Langmuir, and (e) Freundlich.	35
Figure 17 Parity plot of fitted Freundlich isotherm model for adsorption of n-hexane on NORIT RB 4 activated carbon.	36

LIST OF TABLES

Table 1 Physical data of ethylbenzene and n-hexane	5
Table 2 Representation of the difference between physical adsorption and chemisorption	7
Table 3 The pores sizes according to the IUPAC	8
Table 4 Textural properties of the NORIT RB4 adsorbent.	25
Table 5 Textural properties of NORIT RB4 measured by H2 adsorption at 77.35 K.	26
Table 6 Characteristics of NORIT RB4 measured from mercury porosimetry studies.	26
Table 7 Adsorbent and column properties.	28
Table 8 Fixed bed experimental conditions for single component adsorption of ethylbenzene and n-hexane on Norit RB4 AC and respective loading for each run.	31
Table 9 Parameters of the different adsorption models for ethylbenzene and regression coefficients.	33
Table 10 Parameters of the different adsorption models for n-hexane.	35

NOMENCLATURE

b	Adsorption equilibrium affinity constant (bar^{-1})
b_0	Pre-exponential factor of the affinity constant (bar^{-1})
C_0	Feed gas concentration at the inlet of the fixed bed (mol.m^{-3})
d_p	Pellet diameter (\AA)
F	Feed molar rate of adsorbate at the outlet of the bed ($\text{mol.m}^{-2}.\text{s}^{-1}$)
F_0	Feed molar rate of adsorbate at the inlet of the bed ($\text{mol.m}^{-2}.\text{s}^{-1}$)
g	Redlich-Peterson adsorption isotherm exponent (-)
K	Freundlich adsorption isotherm constant ($\text{mol.kg}^{-1}.\text{bar}^{-1}$)
L	Length of column (m)
M	Molar weight of adsorbate (g.mol^{-1})
m_{ads}	Mass of adsorbent inside column (g)
m_p	Mass of adsorbent particle (g)
n	Adsorption intensity constant of Freundlich isotherm (-)
N_A	Avogadro number ($6.022 \times 10^{23} \text{ mol}^{-1}$)
p	Partial pressure of adsorbate (bar)
P_0	Saturation vapor pressure of adsorbate (bar)
P	Total pressure of column (bar)
q	Amount adsorbed (mol.kg^{-1})
q_{cal}	Calculated amount adsorbed (mol.kg^{-1})
$\overline{q_{\text{cal}}}$	Average calculated amount adsorbed (mol.kg^{-1})
q_{exp}	Experimental amount adsorbed (mol.kg^{-1})

q_{\max}	Maximum amount adsorbed (mol.kg^{-1})
R	Universal gas law constant ($8.314 \text{ J.mol}^{-1}.\text{K}^{-1}$)
S_g	Specific surface area ($\text{m}^2.\text{g}^{-1}$)
t	Heterogeneity constant of Toth isotherm (-)
t_0	Reference heterogeneity constant (-)
t_{∞}	Bed saturation time (s)
T	Temperature (K)
v	Volume of adsorbed gas (cm^3)
V_c	Column volume (m^3)
V_{He}	Volume of helium displaced by the adsorbent (m^3)
V_{Hg}	Volume of mercury displaced by the adsorbent (m^3)
V_m	Volume of monomolecular layer of gas adsorbed at STP (cm^3)
V_g	Specific pore volume ($\text{cm}^3.\text{g}$)

Greek letters

α	Surface area covered per adsorbed molecule (-)
ΔH_{ads}	Heat of adsorption (kJ.mol^{-1})
ΔH_{cond}	Heat of condensation (kJ.mol^{-1})
Δq	Error between theoretical and experimental amount adsorbed (-)
ε_p	Particle porosity (-)
ε_b	Bed porosity (-)
ρ_L	Adsorbate density in liquid phase (g.cm^{-3})
ρ_P	Particle density (g.cm^{-3})

ρ_s True pore density ($\text{g}\cdot\text{cm}^{-3}$)

Abbreviations

AC Activated carbon

BET Brunauer, Emmet and Teller

IUPAC International Union of Pure and Applied Chemistry

MFC Mass Flow Controller

SEM Scanning Electron Microscope

TCD Thermal Conduct Detector

VOCs Volatile Organic Compounds

INTRODUCTION

Volatile Organic Compounds (VOCs) can be defined as a collection of chemical species, often solvents, that tend to evaporate at room temperature [1]. The VOCs can be classed in several groups based on their properties such as the boiling point, the molecular structure, and the molecular polarity. For the molecular structure, the VOCs include alkanes, alkenes, aromatic hydrocarbons, alcohols, aldehydes, ketones etc. Moreover, the polar and nonpolar VOCs are distinguished according to the degree of molecular polarity [2,3,4]. Figure 1, shows the classification of most common VOCs [5].

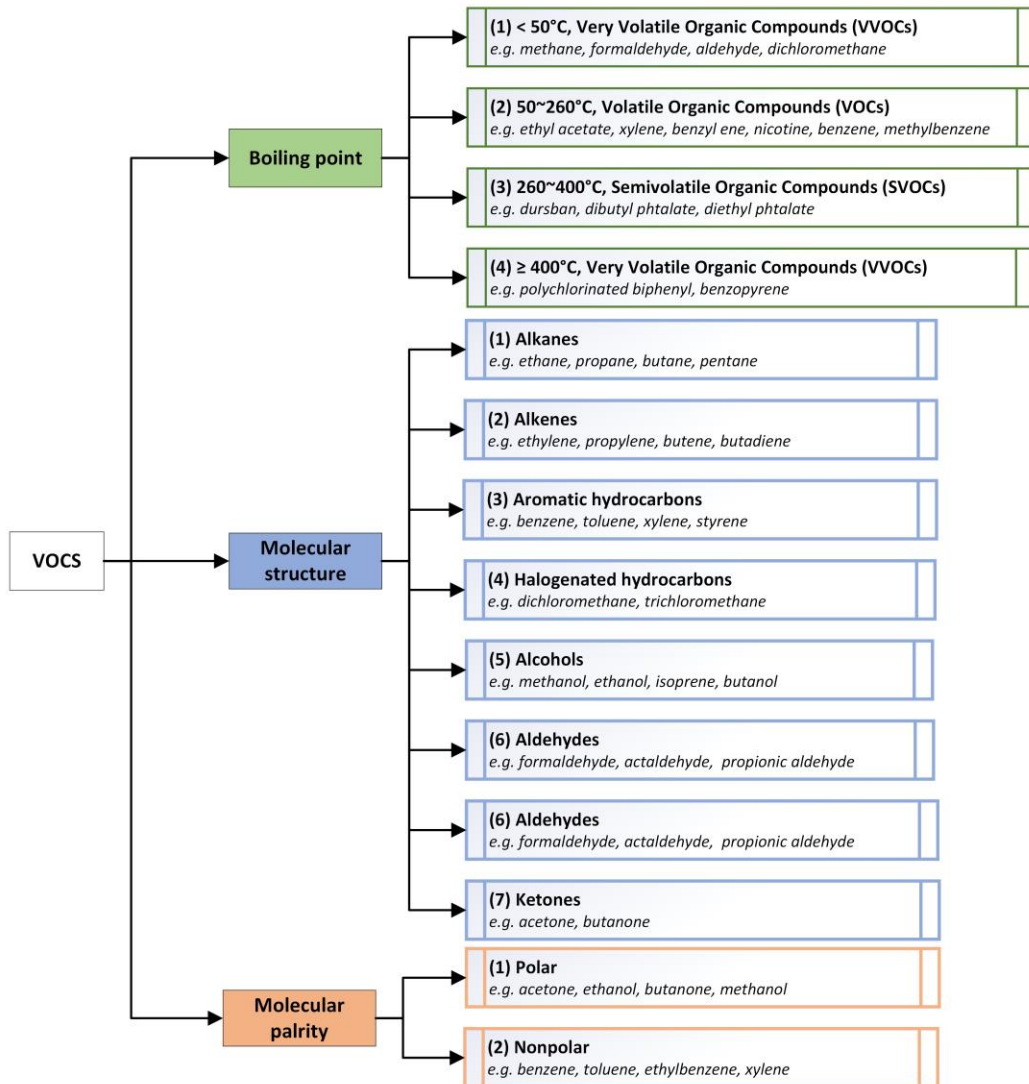


Figure 1 Classification of different VOCs [5].

Since VOCs are essentially solvents, they are therefore widely used at various levels in industrial processes. This has the consequence of resulting in a wide dissemination of VOCs in the environment. The emission of biogenic origin VOCs represents over 90% of the total amount of VOCs entering the atmosphere [6]. In addition, with the accelerated industrialization and economic growth, the annual emission of VOCs in recent years increases dramatically, especially in the developing countries as China. The emission amount of VOCs from anthropogenic sources in China are predicated to be persistently increased above 5.9% [7]. As shown in the figure 2, industrial processes, in particular petrochemical, chemical engineering, coating and printing industries, accounted for 43% of the anthropogenic origin of VOCs in China during 2015 [8].

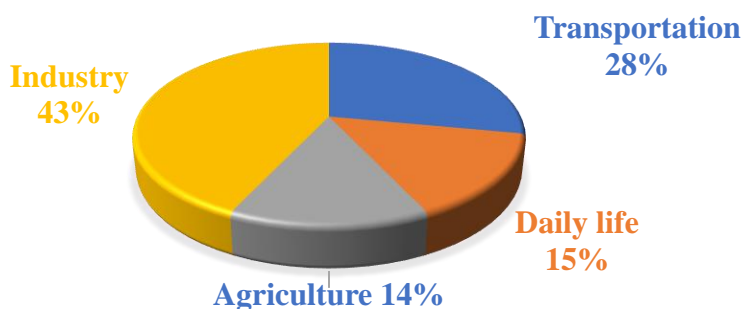


Figure 2 VOCs emission from different sources in China in 2015 [8].

VOCs pose a serious threat to ecological environment and human health because they are highly toxic and carcinogenic and hazardous [9]. As for the human health, most VOCs are a significant contributor to sick building syndrome [10]. In enclosed spaces, VOCs cause irritation to eye, nose, and throat, and more severely cause dizziness, headache, memory and visual impairment and even death [11]. Besides the damages to humans, VOCs are major contributors to stratospheric ozone depletion and regional ozone formation. Evaporated alkanes, aromatic compounds and alkenes undergo photochemical reactions under suitable climatic conditions [12- 14]. The species with the highest ozone formation potential, including m/p-xylene, toluene, propene, o-xylene, and ethyl benzene, account for 30% of the total VOCs emissions, resulting in 69% of the total ozone production potential (OFP) [15]. With the persistent increase of VOCs emission, many techniques to the degradation of VOCs are being investigated and applied. The classification of VOCs degradation methods is shown in the Figure 3 [16].

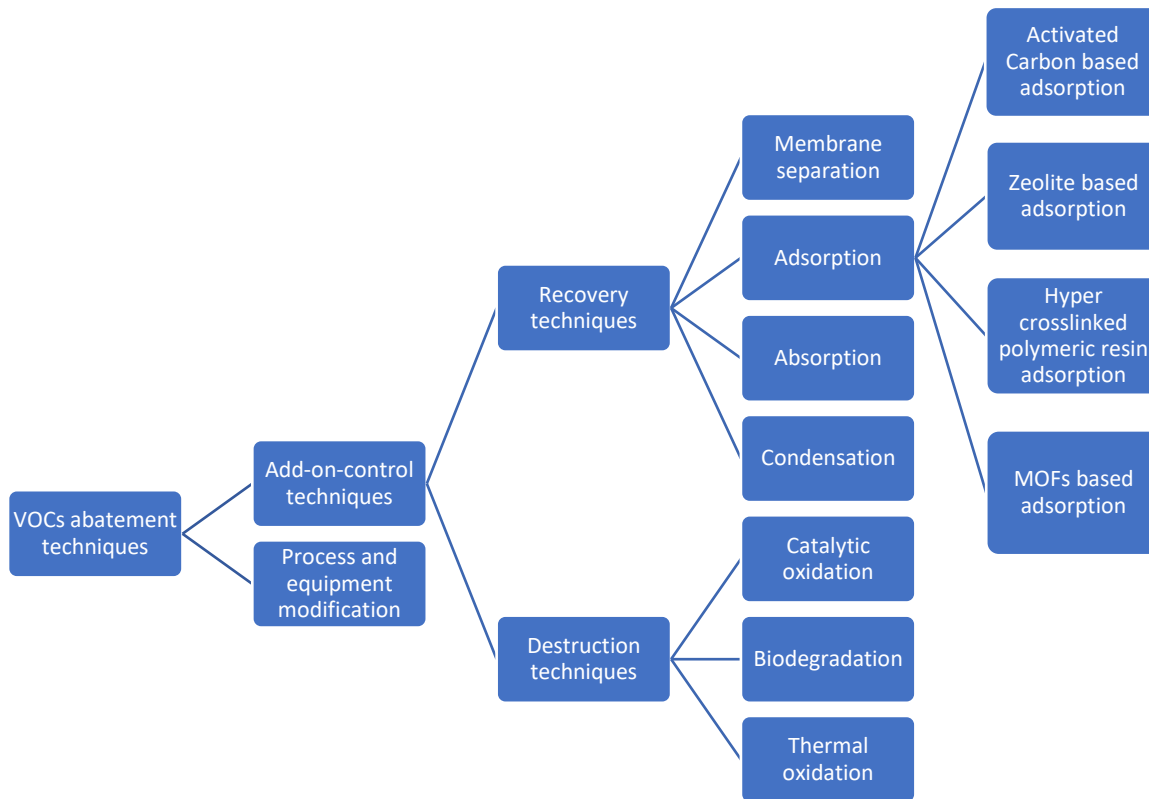


Figure 3 Classification of VOCs degradation methods [16].

The adsorption is one of the most widely used method for the removal of VOCs, especially using activated carbon, due to its abundance and low-cost manufacturing. Activated carbon also exhibits a good adsorption capacity for VOCs [8].

This work aims to study the capability of using commercial activated carbon for the removal of two very important VOCs from air streams namely, ethylbenzene and n-hexane. For that a chromatographic technique to measure the adsorption isotherms in relevant temperature and partial pressure conditions generally observed in the emission of these compounds through air streams is applied. The chromatographic technique is based in the measurement of breakthrough curves from where a mixture of the VOCs in air is introduced in a fixed bed containing the pellets of activated carbon. Data treatments allow the measurement of the sorption uptake and different temperatures and partial pressures conditions with the respective set-up of the adsorption equilibrium isotherms, fundamental for the design of the technological applications for the removal of VOCs by adsorption processes.

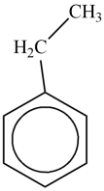
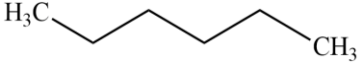
1. STATE OF THE ART

1.1 Harmfulness of volatile organic compounds

One of VOCs that attracts attention is the aromatic compounds of BTEX family (benzene, toluene, ethylbenzene, and xylene) which are very often associated with human health problems. They come mainly from the crude oil and natural gas industry, obtained through various chemical reactions (alkylation, dealkylation ...). Once they have been synthesized or isolated there, they will be used in various industries such as inks, pesticides, fuels, detergents, and paints. Their use can be limited to the laboratory scale where they can, among other things, be used as a solvent in various extractions or for the synthesis of other chemicals and pharmaceuticals. Their presence on all sides means that they are largely released into the environment whether by their combustion or from domestic use. The BTEX that will interest us is the *ethylbenzene*, which is a benzene compound having an ethyl group. It has been established that exposure to ethylbenzene causes adverse effects on its in humans development because it causes a drop in birth rate, it also impacts immunological function (atopy, rhinitis) but also respiratory function because it can be the cause of asthma [17].

Another category of VOCs that requires attention are the aliphatic hydrocarbons, more specifically, the alkanes found in fuels. They are also derived from the crude oil industry and harmful to the human health. For this family, we will bring our attention to the *n-hexane*, which is known as the most toxic member of the alkanes. It is used on a laboratory scale in extraction operations in various environments, it is also a solvent, a cleaning agent and diluent. Exposure to n-hexane most often in its vapor form, mainly occurs through the respiratory route but also through the dermal route. This exposure has been shown to disturb the nervous system, leading to a slowdown in brain function and muscle weakening, among other things. The toxicity of n-hexane causes a reduction in immunoglobulins [18]. Table 1 resume the properties of ethylbenzene and n-Hexane.

Table 1 Physical data of ethylbenzene and n-hexane [19,20].

	ethylbenzene	n-hexane
Chemical formula	C ₈ H ₁₀	C ₆ H ₁₄
Structure		
Molar mass (g/mol)	106.17	86.18
Boiling point (°C)	136.1	69
Melting point (°C)	-94.9	-95
Water solubility (mg/mL) at 25°C	0.152	9.5
Vapor pressure (mm Hg) at 25°C	7.5	150
Density (g/mL) at 20°C	0.867	0.66

1.2 Adsorption

Adsorption is a process in which certain chemical species present in a fluid phase called Solute or *Adsorbate* are transferred onto or near the surfaces or pores of a solid called *Adsorbent*. During this process weak intermolecular forces can occur between the atoms/molecules/ions and the surface of the Adsorbent, otherwise these species diffuse to the surface of the Adsorbent. When the bond which occurred between the adsorbate and the adsorbent is the result of *London-van der Waals* forces, it is called a *physical adsorption*. But if the adsorption take place through chemical bonding forces, this adsorption is referred to as *chemisorption*.

To achieve a substantial adsorption area per unit volume, highly porous solid particles with interconnected pores of small diameter are used, most of the adsorption occurring inside the pores. During adsorption the sorbent will be saturated or nearly saturated with molecules of the adsorbate. In order to reuse the adsorbent and recover the adsorbed substances, the solid is regenerated by a *desorption* of the adsorbed substances [21].

1.3 Physical adsorption and chemisorption

Generally, adsorption can be classified in different ways, it can be classified as physical or chemical adsorption on the basis of the magnitude of the heat of the adsorption. Although such an approach is widely used because of its convenience, it is not very precise [22]. It can also be classified as mobile or immobile adsorption from the molecular point of view. Nonetheless, it can be classified as monolayer or multilayer depending on the magnitude of the relative pressure [23].

Physical adsorption for a gas phase takes place when the intermolecular forces between the sorbent and the molecules of the gas are more significant than those between molecules of the gas itself. It should be noted that this kind adsorption is exothermic, here the magnitude of the heat released can be less or more than the vaporization's heat. The physical adsorption energy range is 2-10 kcal/mol. For chemisorption, there is a direct chemical bond between the sorbent and the adsorbate. The energy of this adsorption is of the same order of the magnitude as the energy change in a comparable chemical reaction, this energy range is 15-100 kcal/mol. In general Chemisorption from a gas stream occurs at temperatures greater than 200°C and can be slow and irreversible. When a molecule adsorbed by chemisorption loses its identity on reaction or dissociation and cannot be regenerated by desorption, a molecule adsorbed by physical adsorption generally preserves its identity moreover on desorption it returns to its original form. Another disparity point between these two ways of adsorption is that chemisorption is restricted to a monolayer, while physical adsorption usually takes place for multilayers at relatively high pressures [23].

The main characteristics allowing to differentiate chemisorption from physical adsorption are presented in table 2.

Table 2 Representation of the difference between physical adsorption and chemisorption [24].

Physical Adsorption	Chemisorption
Monolayer or multilayer	Monolayer
No electron transfer	Electron transfer leading to bond formation between sorbate and sorbent
Low heat of adsorption (<2 or 3 times latent heat of evaporation)	High heat of adsorption (>2 or 3 times latent heat of evaporation)
Adsorbed species regenerated	May involve dissociation
Only significant at relatively low temperature	Possible over a wide range of temperature
Nonspecific	Highly specific
Rapid non-activated Reversible	Activated, may be slow and irreversible

1.3.1 Mobile and Immobile Adsorption

In the case of mobile adsorption, a molecule can move while it is adsorbed on the surface, that is, this molecule remains in the adsorbed state all the time. In the case of immobile adsorption, a molecule does not leave its adsorbed location before desorbing and returning to the fluid phase. It is important to note that localized adsorption behaves like stationary adsorption, whereas a non-localized molecule can be mobile. In general, the adsorbed molecules occupy fixed locations, but in some cases, they are free to move from one position to another [22].

1.3.2 Monolayer and Multilayer Adsorption and Capillary Condensation

The amount of physically adsorbed gas molecules always decreases monotonically as temperature increases. The amount is usually associated with the relative pressure, P/P_0 , where P and P_0 are the partial vapor pressure of a component in the system and the saturation vapor pressure at the same temperature, respectively. For example, when the relative pressure is about 0.01 or less, the amount of physical adsorption for nonporous materials can be considered negligible. However, this is not true for microporous solids such as active carbon. For $P/P_0 \approx 0.1$, the amount adsorbed corresponds to a monolayer. The monolayer capacity is usually defined as either the chemisorbed amount required to occupy all surface sorption sites or the physisorbed amount required to cover the surface. As the pressure increases progressively, multilayer adsorption occurs until a bulk

liquid is reached at P/P0) 1.0. The approximate values of relative pressure for multilayer adsorption range from 0.1 to 0.3, beyond which pores are filled with a liquid like phase. This phase transition is known as capillary condensation. It is noteworthy that these concepts should apply only for conditions below the critical point [23].

1.4 Adsorbents

The four types of adsorbents dominating the market are: activated carbon, zeolites, silica gel, activated alumina. Activated alumina and silica gel are mainly used as desiccants, although they exist in many modified forms available for special cases. Zeolites are used for their special adsorption properties due to their unique surface chemistries and crystalline pore structures. Activated carbon is used as an all-purpose adsorbent, it is a hydrophobic material [24]. In order to characterize an adsorbent, various parameters must be considered:

They are classified on the basis of their geometries, generally they are shaped as cylindrical, granules, spherical pellets, flakes, or powders with sizes ranging from 50 μm to 1.2 cm. On the other hand, they are classified according to the size of their pores. In fact, according to the classification of the International Union of Pure and Applied Chemistry (IUPAC) they are classified as shown in the table 3.

Table 3 The pores sizes according to the IUPAC [25].

Type	Pores sizes (Å)
Micropore	<20
Mesopore	20-500
Macropore	>500

The monolayer coverage allows us to determinate the surface area. The covered zone can be calculated by considering the amount of gas used from the monolayer as well as the dimensions and the number of molecules. Even if there are a lot of methods in use, the most prevalent and used is the BET equation (Brunauer, Emmet, and Teller) based on the BET method for gas adsorption onto a solid surface. It consists in the adsorption of Nitrogen -195.8°C (boiling point of

N₂) by measuring the volume of N₂ adsorbed in a few grams of adsorbent at different pressures, generally between 5 and 250 mmHg [26]. It assumes that the heat of adsorption during monolayer formation (ΔH_{ads}) is constant and the heat effect associated with subsequent layers is equal to the heat of condensation (ΔH_{cond}) [21].

The BET equation is given by:

$$\frac{P}{v(P_0 - P)} = \frac{1}{V_m c} + \frac{c - 1}{V_m c} \left(\frac{P}{P_0} \right) \quad (1)$$

where P is the total pressure, P₀ the vapor pressure of adsorbate at test temperature, v the volume of gas adsorbed at STP (0°C; 760mmHg), V_m the volume of monomolecular layer of gas adsorbed at STP and C the constant related to the heat of adsorption. A plot of $p / [v (P_0 - P)]$ as ordinate and (P/P_0) as the abscissa, permit to determinate V_m and the C from the slope and the intercept of the best straight line fit to the data. Accordingly, we can obtain:

$$Slope = \frac{c - 1}{V_m c} \quad (2)$$

$$intercept = \frac{1}{V_m c} \quad (3)$$

Which in terms gives:

$$V_m = \frac{1}{Slope + intercept} \quad (4)$$

From where the specific surface area S_g can then be derived:

$$s_g = \frac{\alpha V_m N_A}{v} \quad (5)$$

With N_A is the Avogadro's number (6.022 x 10²³ mol⁻¹) and v is the volume of gas adsorbed per mole at STP (22,400 dm³/mol).

The quantity α is the surface area covered per adsorbed molecule. If we assume spherical molecules arranged in close-dimensional packing; the projected surface area is:

$$\alpha = 1.091 \left(\frac{M}{N_A \rho_L} \right)^{\frac{2}{3}} \quad (6)$$

Where M is the molecular weight of the adsorbate (in mol/g) and ρ_L is the density of the adsorbate taken as the liquid at the test temperature (in g/cm³).

In addition, the specific pore volume Vg , generally in cm³ of pore volume per gram of adsorbent, is determined for small mass of adsorbent m_p , by measuring the volumes of helium, V_{He} , and mercury, V_{Hg} , displaced by the adsorbent. The helium is not adsorbed but fills the pores. At ambient pressure, the mercury cannot enter the pores because of unfavorable interfacial tension. The specific pore volume, Vg , is then determined from:

$$Vg = \frac{(V_{Hg} - V_{He})}{m_p} \quad (7)$$

The particle density is obtained from:

$$\rho_p = \frac{m_p}{V_{Hg}} \quad (8)$$

The true pore density is obtained from:

$$\rho_s = \frac{m_p}{V_{He}} \quad (9)$$

The distribution of pore volume over the range of pore size, which is of great importance in adsorption, is measured by mercury porosimetry for large-diameter pores (> 100 Å); by gaseous-nitrogen desorption for pores of 15-250 Å in diameter; and by molecular sieving, using molecules of different diameter, for pores < 15 Å in diameter. In mercury porosimetry, the extent of mercury penetration into the pores is measured as a function of applied hydrostatic pressure [23].

The fundamental relation is:

$$d_p(\text{\AA}) = \frac{21.6 \times 10^5}{P} \quad (10)$$

where P (in psia) is the pressure required for the mercury enter into the pores of the adsorbents.

For a target adsorbate molecule, the selection or synthesis of adsorbents is based on the adsorption isotherm. This one can be calculated by using: the geometry/structure of the adsorbent and the interaction potentials. With a few quantities of adsorbent, we can obtain huge surface area due to the particle porosity from 30 to 85 vol% with average diameters from 10 to 200 Å [26].

To determinate the specific surface area S_g let's consider a cylindrical pore of diameter d_p and length L (in m), then the surface area-to-volume ratio is:

$$\frac{S}{V} = \frac{\pi d_p L}{\pi d_p^2 \frac{L}{4}} = \frac{4}{d_p} \quad (11)$$

Where S and V are respectively the surface (in m²) and the volume (in m³) of a single pellet,

Then, as ε_p is the particle porosity and ρ_p the particle density, then the specific surface area is:

$$S_g = \frac{4\varepsilon_p}{\rho_p d_p} \quad (12)$$

1.5 Activated carbon

Activated carbon also called activated charcoal is the most widely used sorbent for the removal of VOCs because it is hydrophobic and has a high specific surface area. It is manufactured from carbonaceous raw material such as wood, petroleum coke, bones, coconut shell, and fruit nuts. These raw materials must be low in inorganic matter, available and cheap. Their degradation must be low even during storage. They should be easily activated; this activation consists of two different essential stages: *carbonization* and *activation* [26].

Carbonization is the heat treatment or pyrolytic decomposition of the raw material in the absence of oxygen at temperatures in the range of 400-900°C. During this step the impurities such as oxygen, hydrogen, nitrogen, and sulfur are consequently removed, then the product obtained is

called *Char*. The *Char* does not have a high adsorption capacity yet because its pores structure is not fully pronounced. Therefore, this pore structure must be perfected by an oxidative treatment called activation. The activation process is based on the destruction of the carbon structure by oxidation of the carbonized material, which will produce a highly porous structure consisting largely of micropores. This process consists to expose the *Char* to an oxidizing atmosphere based on gases such as air, steam, carbon dioxide or their combination in a range of temperature of 500-1000°C, thus a *thermally activated carbon* is obtained [26].

In the other hand the raw material can be impregnated with dehydrating and oxidizing chemicals such as phosphoric acid and zinc chloride, then the impregnated material is pyrolytically heated to temperatures of 400-800°C, here the carbonization and the activation occurs at the same time, thus *chemically activated carbon* is obtained. The figure 4 below resumes the steps of the production of Activated carbon [27].

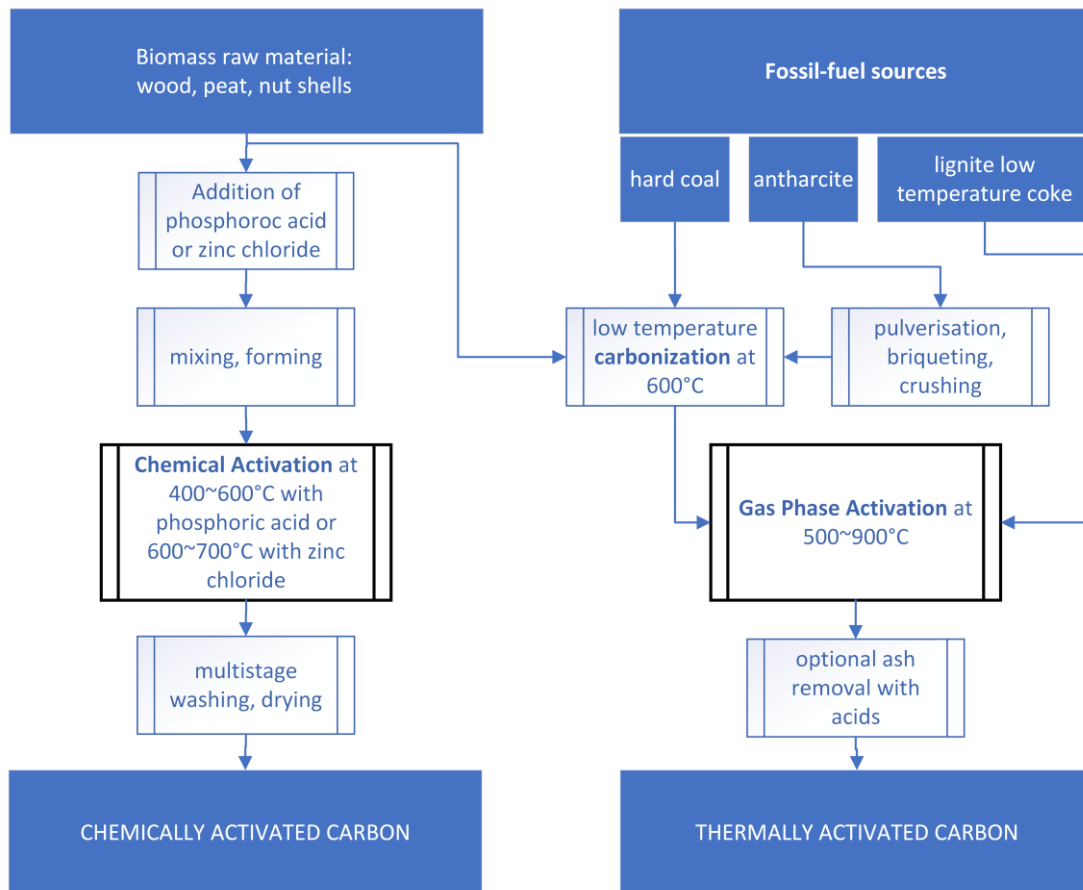


Figure 4 Production of Activated Carbon [27].

It would then be relevant to manufacture an activated carbon based on organic residues such as the green coconut shell and then to gauge its effectiveness by comparing it to the activated carbon obtained from pine wood which has a BET surface area in the range of 426~902 m²/g [28].

Indeed, it has been shown that activated carbon in the form of fibers, granular, cloth or pellets were effective for the removal of VOCs through adsorption process. Different types of raw materials, such as coconut shell, wood or mesophase pitch are used to synthesize activated carbon for the VOCs adsorption [29].

1.6 Adsorption isotherms

An adsorption isotherm represents the amount adsorbed per unit weight of adsorbent as a function of the adsorbate(solute) partial pressure or concentration in bulk fluid phase at equilibrium [25]. When a sorbate gas is adsorbed onto a previously unoccupied solid surface or its pore space, the amount of gas adsorbed is proportional to the solid mass. The adsorption of the gas also depends on the temperature (T), the equilibrium partial pressure of the vapor (p) and the nature of the solid and the gas. For a gas adsorbed on a solid at a fixed temperature, the quantity adsorbed per unit mass of the solid (q) is then only a function of p . The relationship between q and p at a given temperature is called the adsorption isotherm. q is frequently presented as a function of the relative pressure [30]. As described in figure 4, there are six principal classes of adsorption isotherms, from types I to VI.

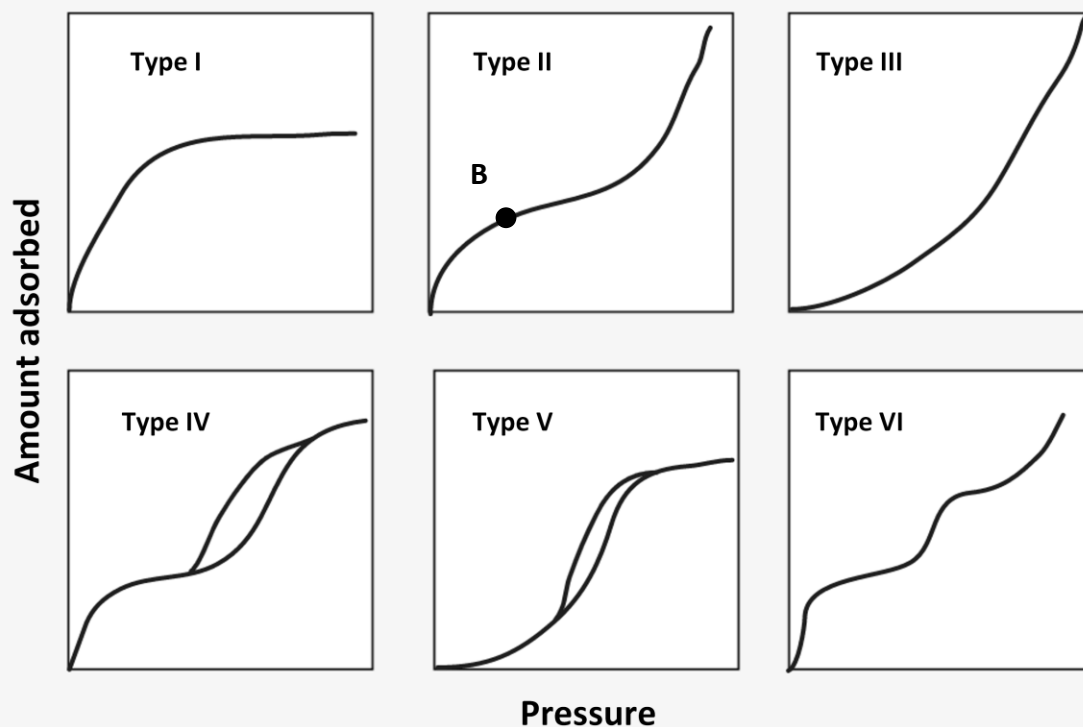


Figure 4 The shape of the five type of adsorption isotherms according to the IUPAC [31].

1.6.1 Type I isotherm

It is the simplest one, it corresponds to a unimolecular adsorption, characterized by a maximum limit in the amount adsorbed. This limit corresponds to the theoretical completion of a surface monolayer. This type of adsorption is often done for gases at temperatures above their critical temperature [22].

1.6.2 Type II isotherm

This type of isotherm is commonly used for physical adsorption on more or less open surfaces, in which the adsorption takes place gradually from sub-monolayer to a multilayer. The isotherm has a distinct concave descending curvature at some low relative pressure p and a strongly ascending curve at high p . Point B of the curve corresponds to the filling of an adsorbed monolayer. This is the basis of the Brunauer - Emmett - Teller (BET) model for determining the area of a solid from the monolayer capacity [30].

1.6.3 Type III isotherm

The type III isotherm stands out by being convex to the relative pressure axis, which causes a weak extent of adsorption in the lower pressure. This type of isotherm signifies a relatively weak gas–solid interaction. In this case, the adsorbate does not effectively spread on the solid surface [30].

1.6.4 Type IV and V isotherms

These types of adsorptions are characteristic of vapor adsorption by capillary condensation into small adsorbent pores. In these types of adsorptions, the adsorption reaches an asymptotic value as the saturation pressure is approached [30].

1.6.5 Type VI isotherm

The type VI isotherm, characterized by multiple stages is a representative of an adsorption in several stages. This is the only type not appearing in the classification of Brunauer [31].

2. EXPERIMENTAL SECTION

2.1 Measurement of gas adsorption isotherms in a fixed bed by chromatography

2.1.1 Chromatographic technique

In order to measure adsorption equilibria isotherms, gas chromatography is often used. In addition, it is the most effective technique for the detection of BTEX in the air [32]. In fact, a non-adsorbing gas is mixed with the adsorbable species (previously pulverized if it is liquid); this mixture is brought into contact with the adsorbent to be studied previously placed in a fixed bed. At first the fixed bed is free from any adsorbate, as the gas mixture passes through the column the adsorbate is retained by the adsorbent until is completely saturated. At this time, the solute concentrations at the column inlet and outlet are identical. The chromatogram resulting from this type of chromatographic experiment is called a breakthrough curve. The figure 5 describes the adsorption process and the corresponding breakthrough curve to be observed [33].

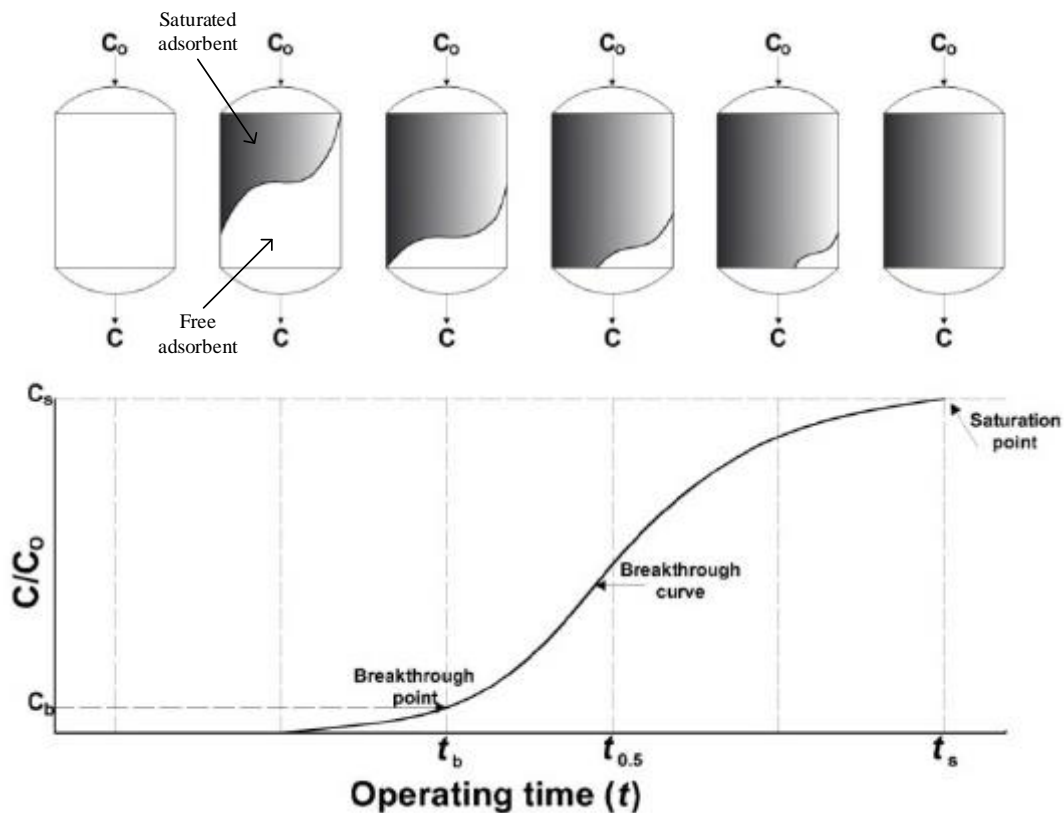


Figure 5 Schematic representation of the fixed bed adsorption and the corresponding observed breakthrough curve [33].

2.1.2 Breakthrough Curves

After the experimentation, one obtains a breakthrough curve concentration profile. Normally, ideal adsorption results in S-shaped breakthrough curves. A simple integration along this curve as indicated in the figure below makes it possible to determine the quantity adsorbed. Figure 6 represents the area integrated for the calculation of the sorption uptake.

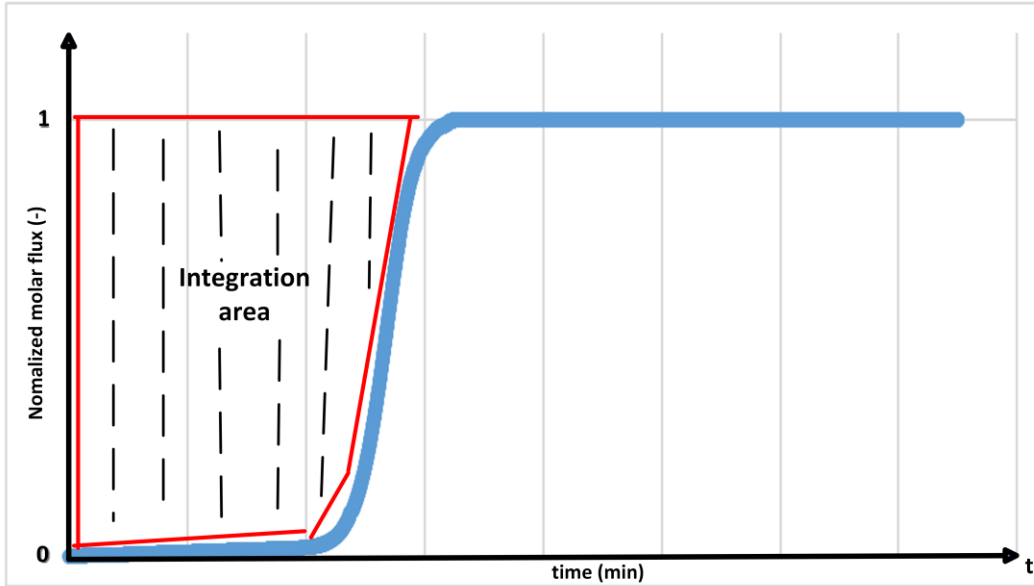


Figure 6 Representation of the integrated area in the breakthrough curve for the calculation of the sorption uptake in a single component experiment.

2.2 Adsorption Equilibrium Isotherm models

2.2.1 Langmuir model

The Langmuir isotherm model is governed by two parameters being compatible with several observed experimental adsorption isotherms (section 1.6.1). It is well suited for the representation of the adsorption equilibrium of single gases in several systems [23,33].

The model is based by the following assumptions:

- Homogeneity of the pores at the surface of the adsorbent
- The adsorption is such that each site can only retain one molecule at a time.
- The interaction forces between adsorbed molecules are negligible
- The adsorption is restricted to a monomolecular layer.
- All sites are energetically equivalent.

For single component adsorption, the model can be noted as[35]:

$$q = \frac{q_{max}bP}{1 + bP} \quad (13)$$

where q is the amount adsorbed, q_{max} is the maximum loading corresponding to complete coverage of the surface by the gas, P is the partial pressure, b is constant defining the affinity of the adsorption on the contact surface.

The integrated equation of Van't Hoff's law represents the effect of temperature on constant b :

$$b = b_0 e^{\left(\frac{-\Delta H}{RT}\right)} \quad (14)$$

where b_0 is the pre-exponential factor, ΔH is the heat of adsorption, R is the ideal gas constant, T is the experimental temperature. Since the adsorption is exothermic, the heat of adsorption is negative, so the constant decreases with the increase in temperature.

2.2.2 Freundlich model

The Freundlich isotherm model is also a widely used model. This also two parameters model was initially designed to describes the adsorption of organic compounds from aqueous streams onto activated carbon, but also in gas phase adsorption of solutes onto activated carbon with heterogenous surfaces [21,33].

The use of this model implies that one assumes that:

- The adsorbent surface is heterogeneous.
- Adsorption is done in patches grouping sites with the same adsorption energy (the amount adsorbed is the sum of all the patches).
- Non-uniform distribution of the heat of adsorption.
- Patches are independent of each other.

The Freundlich model can be represented by the following equation [21]:

$$q = K P^{1/n} \quad (15)$$

where K is a constant related to the capacity of adsorption, n is a constant indicating the adsorption intensity, it is usually in a range of 1 to 5. The more $1/n$ is close to zero, the more the heterogeneity increases. Also, a value above one indicate a cooperative adsorption [36].

2.2.3 Sips model

The Sips model is a combination of the Langmuir and Freundlich isotherms, and it was developed in response to the increasing adsorption amount as a function of pressure predicted by the Freundlich model. Accordingly, we obtain a final empirical isotherm model with a finite adsorption limit at relatively high pressure. Thus, the obtained model is widely used to describe the adsorption of many hydrocarbons onto activated carbon and other adsorbents. When the adsorbate pressure is low the Sips model reduces to a Freundlich isotherm; while at high pressure, it predicts a monolayer adsorption capacity as in the Langmuir model [35,36]. The model is expressed by the following equation [35]:

$$q = \frac{q_{max}(bP)^{\frac{1}{n}}}{1 + (bP)^{\frac{1}{n}}} \quad (16)$$

where q is the amount adsorbed, q_{max} is the maximum amount adsorbed when the adsorbent is saturated, b is the same constant as in the Langmuir model, here also governed by the law of Van't Hoff, n is a constant informing about the heterogeneity of the adsorbent/adsorbate system. So as this parameter increases, the degree of heterogeneity increases.

2.2.4 Toth model

The Toth isotherm model is also effective for describing heterogeneous adsorption systems, whether at low pressures or at high pressure, making this model also a suitable choice to describe adsorption of hydrocarbons, alcohols and carbon oxide onto activated carbon [36].

The equation 17 represent the Toth model for single component adsorption [35]:

$$q = \frac{q_{max}(bP)}{[1 + (bP)^t]^{\frac{1}{t}}} \quad (17)$$

where q_{max} represent the maximum loading of the material, b the affinity constant and P the partial pressure. The parameter t describes the heterogeneity of the system; when equal to one the Toth model turns into Langmuir equation, on the contrary when the value differs from the value one, the system gains in heterogeneity.

The parameters b and t are dependent of the temperature; because b is here also governed by the integrated Van't Hoff equation and the following equation can characterize the relation between the temperature and the affinity constant b :

$$t = t_0 + \alpha \left(1 - \frac{T_0}{T}\right) \quad (18)$$

With T_0 and t_0 respectively the temperature and reference homogeneity parameter, T the experimental temperature and α proportionality coefficient. In the case of experiments at several temperatures, there is an equation that relates the temperature and the maximum amount adsorbed:

$$q_{max} = q_{max,0} \exp \left[x \left(1 - \frac{T_0}{T}\right) \right] \quad (19)$$

With $q_{max,0}$ and T_0 the maximum loading and the temperature at the reference, x is the proportionality coefficient.

2.2.5 Redlich-Peterson model

The Redlich-Peterson adsorption isotherm model is also a hybrid from the Freundlich and Langmuir ones, it has been used in both homogeneous and heterogeneous systems. Its behavior is such that it acts as a Freundlich model when pressure is high and on the contrary when the pressure is low where it approaches the Langmuir model [36].

For a single component, the model is represented by the following equation [38]:

$$q = \frac{q_{max}bP}{1 + (bP)^g} \quad (20)$$

where q_{max} is the maximum amount adsorbed at the saturation of the material of the material, b the affinity constant (following the integrated Van't Hoff equation) and P the partial pressure, the exponent g lies between 0 and 1. When g equals to 1, the model reduces to a Langmuir model and when equals to 0, it turns into a linear model [39].

2.3 The Isotheric heat of adsorption

The isosteric heat describes the heat released during the adsorption phenomenon. It is of a major importance to understand the adsorption strength of the molecules in the adsorbent surface. The heat released by the adsorption of the solute in the adsorption surface causes the temperature of the particles to rise. The Van't Hoff relation described in equation 21 is used to determine isosteric heat [34,39]:

$$\frac{\Delta H_{ads}}{R T^2} = - \left(\frac{\partial \ln P}{\partial T} \right)_q \quad (21)$$

Where R is the ideal gas constant, T the temperature and P the partial pressure

Assuming that the isosteric heat is independent of temperature, for a fixed value of experimental loading by integrating equation (21) in a plot $\ln P$ against $1/T$ we obtain the value of ΔH_{ads} [23]:

$$\ln P = \text{constant} - \frac{\Delta H_{ads}}{R T} \quad (22)$$

In the case where the maximum amount adsorbed depends on the temperature and the latter decreases with temperature, then the heat will increase with loading. Another way of calculating the isosteric heat of two fitted isotherms (with the same model) at two different temperatures, known as the Clausius-Clapeyron approach is then usable [40]:

$$\Delta H_{ads}(q) = -R \cdot \ln\left(\frac{P_2}{P_1}\right) \frac{T_1 T_2}{(T_2 - T_1)} \quad (23)$$

With R as the ideal gas constant. The heat is calculated for a fixed loading q , then for this loading the corresponding temperature and pressure from the two selected isotherms are selected, respectively T_1, T_2 and P_1, P_2 .

2.4 Experimental Apparatus for Measuring Breakthrough Curves

In order to study the adsorption data at equilibrium, the device developed measures the breakthrough curves of a single component in the vapor phase in a fixed bed (dynamic system). Figure 7 describes the schematic diagram. Briefly, the apparatus comprises two main sections: (i) gas preparation and (ii) adsorption column systems.

In the gas preparation section, the helium (ALPHAGAZ 2, 99.9999%, Air Liquide) used as carrier gas (inert) is subdivided into two streams at the system's inlet. The first part, line (1), is routed to the electronic pressure controller (EPC) of the gas chromatograph, while stream (2) goes to a mass flow controller (MFC, MC-100SCCM-D / 5M, Alicat Scientific). At the electronic pressure controller outlet, the stream (1) goes towards the reference side of the Thermal Conductivity Detector (TCD). Meanwhile, the sample to be adsorbed is introduced into a gastight syringe (5MDF-LL-GT, Scientific Glass Engineering) then by using a syringe pump (SP, SP100i, World Precision Instruments), the sample is continuously supplied into the system (in liquid phase) via the stream (3). At the outlet of the MFC, stream (2) goes inside the Gas Chromatograph oven and is mixed with the stream (3). The mixture is then sent into the expansion column (EC, stainless steel with 100 mm of length and 8 mm in internal diameter), within which the vaporization of the adsorbable species in the mixture will take place. At the outlet of the expansion column, the gas mixture flows to a 3-way ball valve (V1, SS-41GXS1, Swagelok), which by default leads to the

bypass line. This bypass is added to ensure the stability of the adsorbate vaporization, and this is before any experiment. The outlet stream of the reference side of TCD is used to dilute the signal of the mixture, a flow metering valve (V2, SS-SS2, Swagelok) is used to control its rate. A manual bubble flowmeter (BF, 10CC EA, Supelco) is placed at the system outlet (TCD exit) to control and control all gas flows.

When the concentration of the adsorbable species previously vaporized gives rise to a constant signal in the TCD, the experiment can be started (adsorption section). When the valve (V1) is opened, the gas mixture from the EC flows through line (4) into the adsorption column (AC, stainless steel with an 84 mm of length and 10 mm in internal diameter), previously filled with activated carbon. The thermal conductivity detector monitors the flow of the adsorbable species coming from the adsorption column throughout the experiment. Also, the signal is recorded in a computer coupled to the gas chromatograph. When the activated carbon is saturated with the adsorbate without changing its composition at the adsorption column outlet, the complete breakthrough curve is measured, marking the end of the experiment. Then the injection via the syringe pump is interrupted, leaving only the gaseous helium through the system, thus cleaning the column (desorption of the sample previously adsorbed).

The experimental set-up is based in a gas chromatograph (SRI 310C, SRI Instruments), which has a forced convection oven to keep the column close to isothermal conditions. The oven temperature and the TCD signal are monitored and recorded, respectively, by PeakSimple data acquisition software (SRI Instruments), a chromatography data system with an intuitive and user-friendly interface.

The panel a) of the Figure 8 shows a realistic view of the experimental apparatus and the panel b) shows closely the inside of the chromatograph oven.

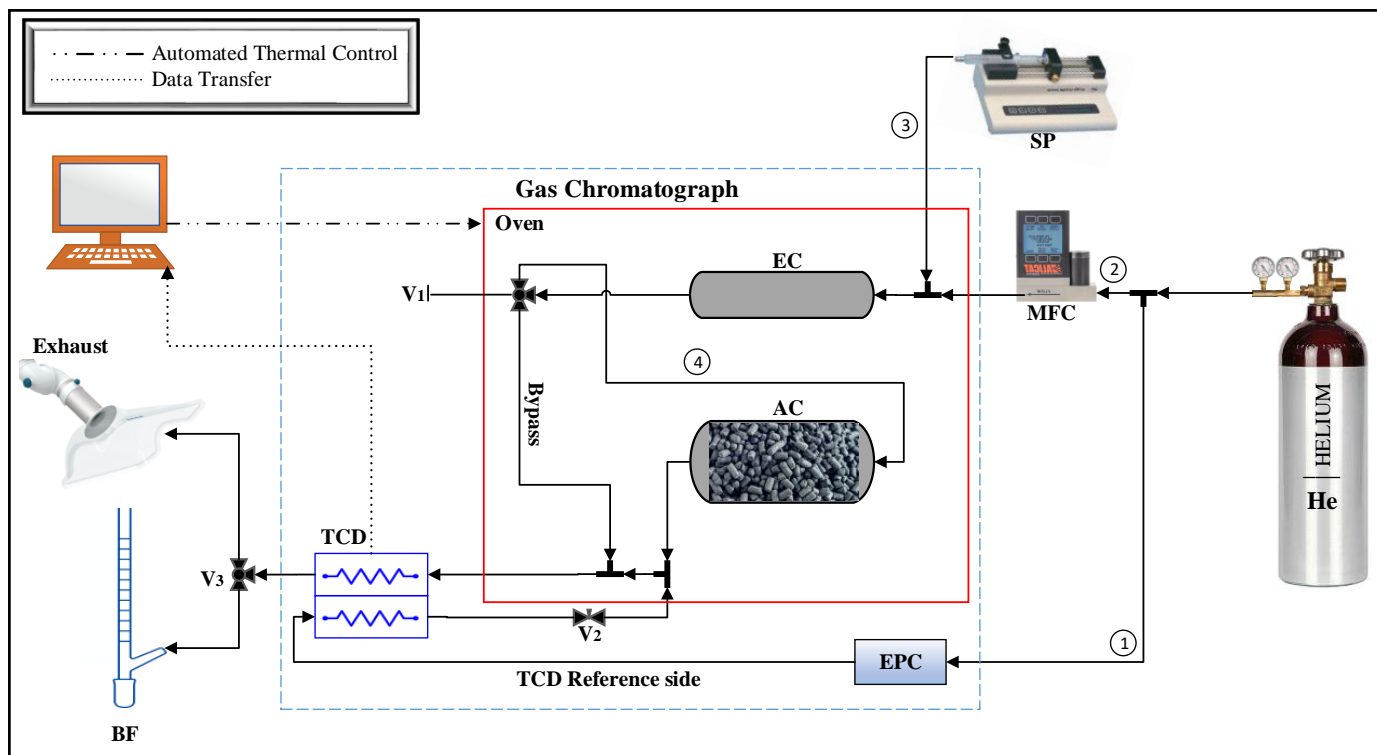


Figure 7 Schematic diagram of the adsorption equilibrium apparatus used to measure adsorption equilibrium data through breakthrough curves: (MFC) mass flow controller; (SP) syringe pump; (AC) adsorption column; (EC) expansion column; (EPC) electronic pressure control; (TCD) thermal conduct detector; (V1) and (V3) 3-way ball valve; (V2) flow metering valve; (BF) bubble flowmeter, and (1)(2)(3)(4) streams.

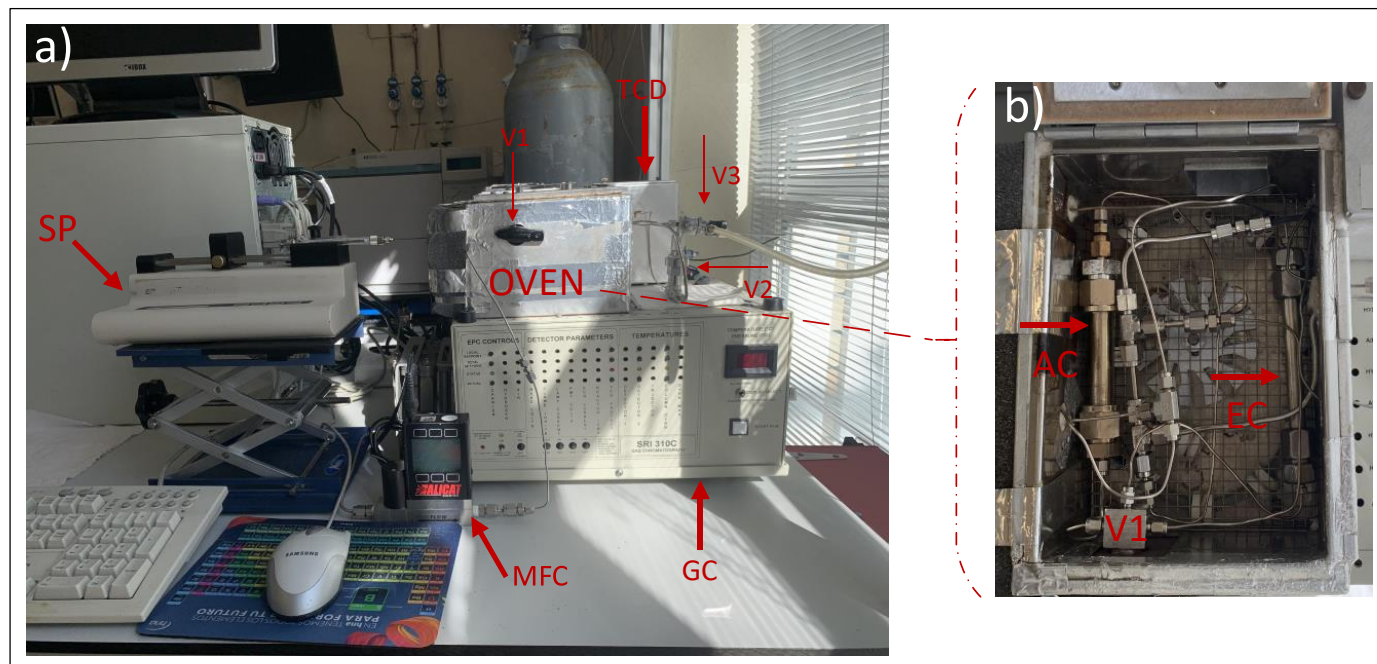


Figure 8 Real view of the chromatographic adsorption equilibrium apparatus: a) detailed view of the overall system, and b) close-up of the inside the chromatograph oven.

2.5 Materials and operating conditions

The adsorbent used in our work is a product kindly provided by Calgon Corporation (USA). The NORIT RB4 (a steam activated extruded carbon) is in shaped cylindrical pellets of 4 mm in diameter. This form of extruded particles reduces the pressure drop. NORIT RB4 is used in gas phase applications requiring high removal yields. Table 4 below shows the properties reported by the manufacturer for NORIT RB4.

Table 4 Textural properties of the NORIT RB4 adsorbent.

Specifications	Values
Total Surface area (B.E.T) (m ² /g)	1100
Apparent density (kg/ m ³)	480
Ash content (mass-%)	9
Moisture as packed (mass-%)	4
Carbon tetrachloride activity (mass-%)	Min. 60
Ball-pan harness (-)	99

In order to obtain more information on this activated carbon, the Laboratorio de Sólidos Porosos of the University of Málaga has kindly carried out analyzes on a sample of NORIT RB 4.

Textural characterization of the NORIT RB 4 sample by Hydrogen (H₂) adsorption at 77.35 K using the Micromeritics ASAP 2420 analyzer, is shown in table 5. Figure 9 shows the adsorption/desorption H₂ isotherm at 77.35 K.

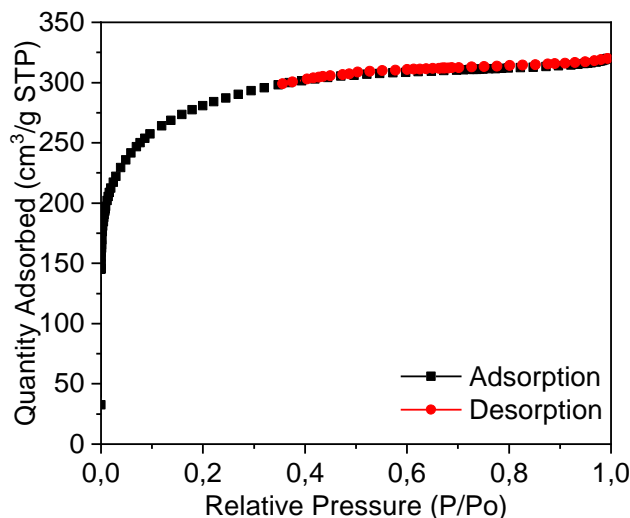


Figure 9 Adsorption/Desorption H₂ isotherm at 77.35 K on activated carbon Norit RB 4 sample for its textural characterization.

Table 5 Textural properties of NORIT RB4 measured by H₂ adsorption at 77.35 K.

Specifications	Values
Langmuir surface area (m ² /g)	1328.5
t-Plot Micropore area (m ² /g)	1257.7
t-Plot External area (m ² /g)	70.9
Total area in pores (m ² /g)	271.9
Total volume in pores (cm ³ /g)	0.574

Analysis of the sample by mercury intrusion in a porosimeter Micromeritics Autopore IV 95000 with the following parameters: contact angle = 130°C, mercury surface tension = 485 dynes/cm and maximum intrusion pressure = 227.5 MPa; allows to obtain the information reported in the following Table 6.

Table 6 Characteristics of NORIT RB4 measured from mercury porosimetry studies.

Specifications	Values
Total intrusion volume (mL/g)	0.3589
Total pore area (m ² /g)	14.06
Median pore diameter (volume) (nm)	1982.4
Median pore diameter (area) (nm)	8.9
Porosity (%)	31.19

The characterization of activated carbon is completed by the micrographs shown in Figure 10, using a scanning electron microscope (SEM).

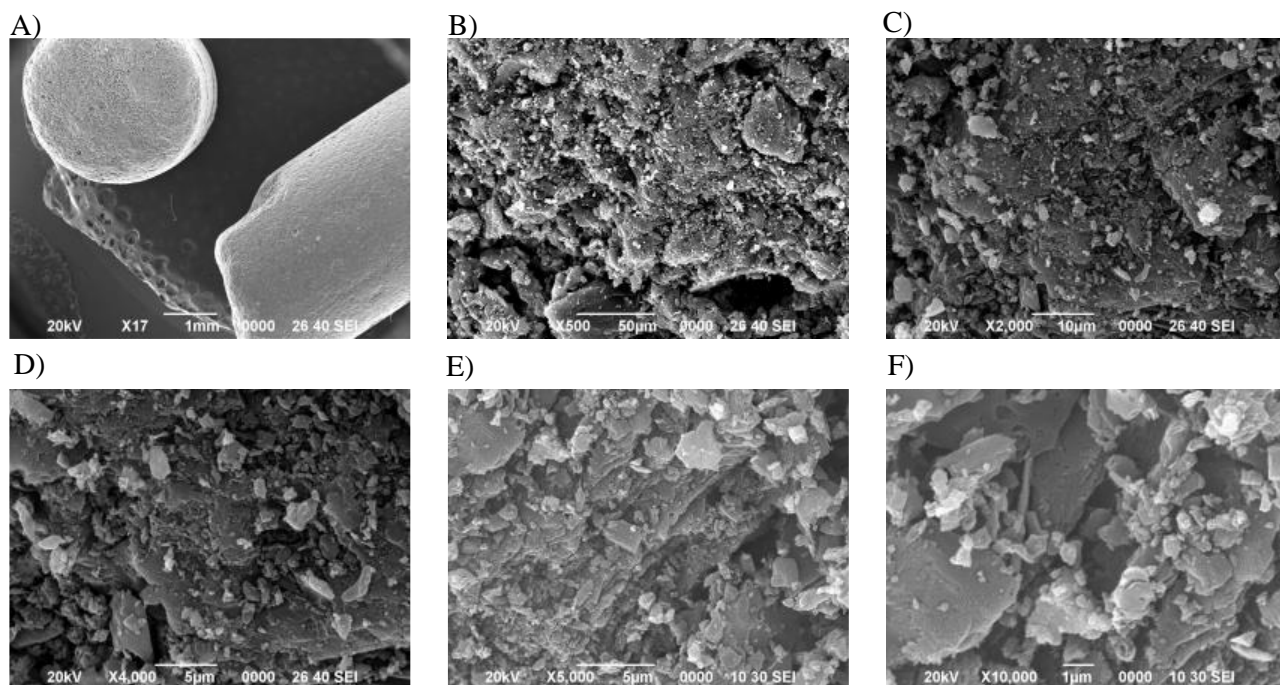


Figure 10 SEM micrographs of the Norit RB 4 activated carbon: Magnified: A)x17, B)x500, C)x2000, D)x4000, E)x5000 and F)x10000

On the first micrograph (A), pores can be seen on the surface of the activated carbon pellets. Then on the following micrography, from (B) to (F), it can be noticed that the sample has a strong heterogeneity in its structure even in the smallest scales (1 μ m).

Several breakthrough experiments were performed which one corresponding to a sorption uptake that gives rise to a point in the adsorption equilibrium isotherm plots. Two compounds were studied: a) ethylbenzene and b) n-hexane. This study was performed at three different temperatures: *i*) 398 K, *ii*) 423 K and *iii*) 448 K, from partial pressures in the range 0.01 to 0.1 bar. Table 7 shows the adsorbent column properties and operating conditions.

Table 7 Adsorbent and column properties.

Parameters	Value	
Total weight of adsorbent in the column	3.088	g
Length	0.091	m
Internal diameter	0.010	m
Area	7.854×10^{-5}	m^2
Volume	7.163×10^{-6}	m^3
Bed porosity	0.4	-

2.6 Experimental procedure

For the studies the column was filled with 3.088 g of the activated carbon (Norit RB4), then it is placed in an oven heated to 473 K for 12 h under a flow of pure Helium (10 mL min^{-1}). When the activation of the adsorbent is completed, the column is placed in the oven and connected to the piping system. Before each experiment, the carrier gas (here helium) is allowed to flow into the system at a controlled flowrate. Then the oven is set to the desired experimental temperature. When the temperature is reached, the injection of the adsorbate, and the experiment can begin. In the end of the experiment the dynamic equilibrium loading is obtained by integrating the molar flow rate profiles of the breakthrough curves by the following equation:

$$q_{exp} = \frac{1}{m_{ads}} \left(F_0 t_n - \int_0^{t_\infty} F dt - \varepsilon_b V_c C_0 \right) \quad (24)$$

Where m_{ads} is the adsorbent mass in the column, F_0 is the feed molar flow rate of adsorbate, F is the molar flow rate of adsorbate in the bulk gas phase, t_∞ is the saturation bed time, ε_b is the bed porosity, V_c is the adsorption column volume and C_0 is the feed gas-phase concentration at the inlet of the fixed bed. The term $\varepsilon_b V_c C_0 / m_{ads}$ represents the adsorbed amount of sorbate gas in the column void space.

3. RESULTS AND DISCUSSION

3.1 Breakthrough curves

Figures 11 and 12 shows respectively all the breakthrough curves measured of ethylbenzene and n-hexane at the three temperatures studied as function of partial pressure of the VOCs. The experimental conditions are given in Table 8.

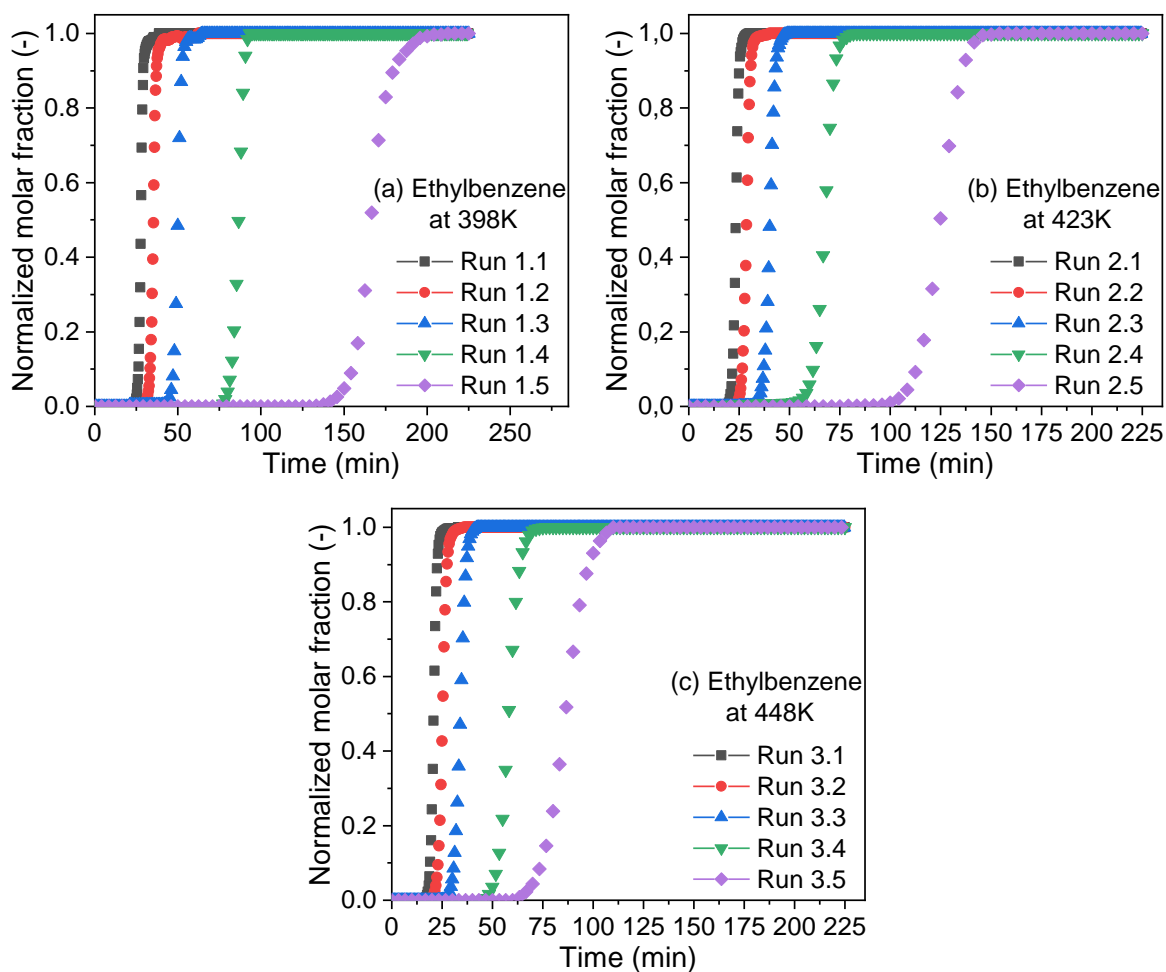


Figure 11 Experimental breakthrough curves of ethylbenzene in activated carbon Norit RB4 at (a) 398, (b) 423, and (c) 448 K and partial pressure up to 0.1 bar. Experimental conditions are given in Table 5.

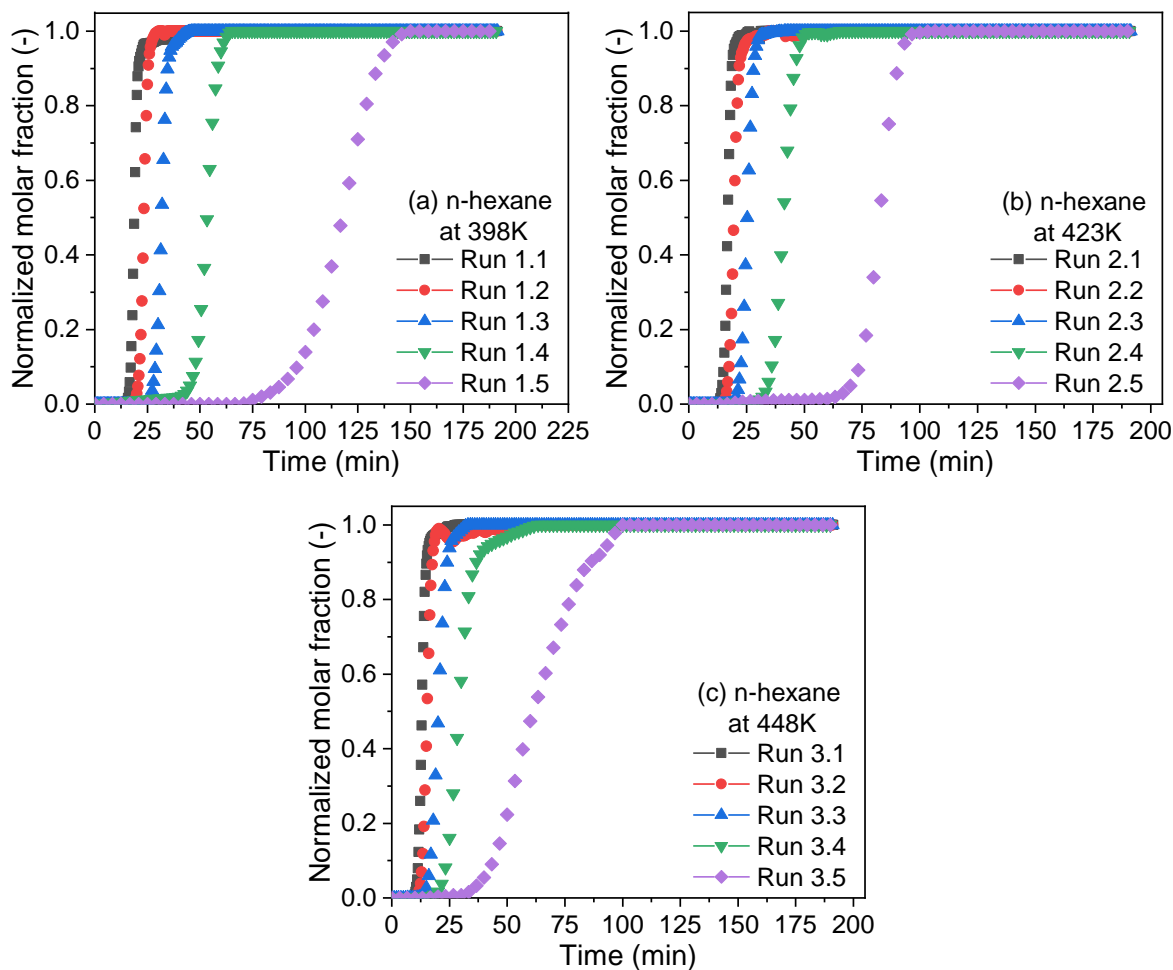


Figure 12 Experimental breakthrough curves of n-hexane in activated carbon Norit RB4 at (a) 398, (b) 423, and (c) 448 K and partial pressure up to 0.1 bar. Experimental conditions are given in Table 5.

Figures 11 and 12 show that for the same adsorbate/solid system, when the temperature increase the time for reaching saturation decreases and consequently the loading as thermodynamically expected for an adsorption process.

The data obtained from the breakthrough curves shown in Figures 11 and 12 allow us to calculate the quantity adsorbed of ethylbenzene and n-hexane by the adsorbent at equilibrium in each test by applying Eq. 24. Thus, in Table 8 are summarized also for each run the values of the equilibrium loading,

Table 8 Fixed bed experimental conditions for single component adsorption of ethylbenzene and n-hexane on Norit RB4 AC and respective loading for each run.

Run	temperature (K)	helium flow rate * (mL/min)	adsorbed specie flow rate * (mL/min)	partial pressure (bar)	loading (mol/kg)
ethylbenzene					
1.1	398	57.8	3.13×10^{-2}	0.100	2.35
1.2		59.8	2.35×10^{-2}	0.075	2.24
1.3		60.8	1.57×10^{-2}	0.050	2.10
1.4		62.6	7.83×10^{-3}	0.025	1.81
1.5		63.7	3.13×10^{-3}	0.010	1.40
2.1	423	54.5	2.95×10^{-2}	0.100	1.85
2.2		56.0	2.21×10^{-2}	0.075	1.71
2.3		57.5	1.47×10^{-2}	0.050	1.59
2.4		59.1	7.37×10^{-3}	0.025	1.33
2.5		54.5	2.95×10^{-3}	0.010	0.99
3.1	448	51.8	2.78×10^{-2}	0.100	1.56
3.2		52.9	2.09×10^{-2}	0.075	1.42
3.3		54.3	1.39×10^{-2}	0.050	1.27
3.4		55.7	6.96×10^{-3}	0.025	1.09
3.5		51.8	2.78×10^{-3}	0.010	0.64
n-hexane					
1.1	398	57.8	3.40×10^{-2}	0.100	1.62
1.2		59.5	2.55×10^{-2}	0.075	1.47
1.3		61.3	1.70×10^{-2}	0.050	1.34
1.4		62.9	8.49×10^{-3}	0.025	1.11
1.5		63.6	3.40×10^{-3}	0.010	0.98
2.1	423	54.6	2.95×10^{-2}	0.100	1.35
2.2		56.0	2.40×10^{-2}	0.075	1.18
2.3		57.4	1.60×10^{-2}	0.050	1.00
2.4		59.2	7.99×10^{-3}	0.025	0.81
2.5		59.8	3.20×10^{-3}	0.010	0.65
3.1	448	51.6	3.02×10^{-2}	0.100	1.00
3.2		52.8	2.26×10^{-2}	0.075	0.91
3.3		54.1	1.51×10^{-2}	0.050	0.76
3.4		55.9	7.54×10^{-3}	0.025	0.56
3.5		56.7	3.02×10^{-3}	0.010	0.47

* Flow rate calculated at 298.15 K and 1 bar.

From the experimental data contained in Table 8, the adsorption equilibrium isotherms can be set-up which are shown in the Figure 13.

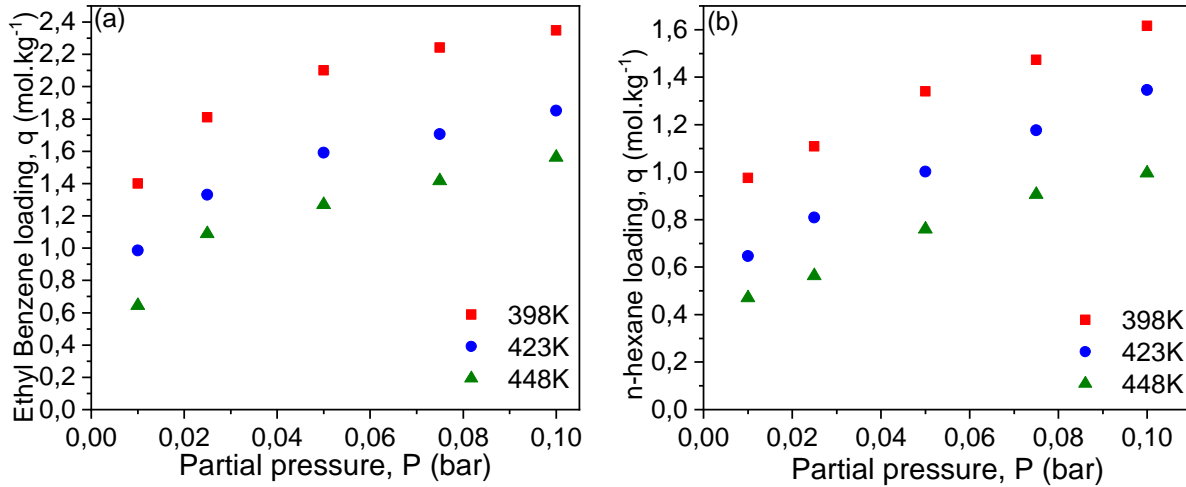


Figure 13 Experimental adsorption equilibrium isotherms of a) ethylbenzene and b) n-hexane on NORIT RB 4 Activated carbon.

For similar experimental conditions, it can be shown in Figure 13 that the loading of ethylbenzene better is higher than the one of n-hexane in the NORIT AC. At the same time and as expected, as the temperature increase the loading decrease, and also the loading increases with the increase of the partial pressure, from where we can conclude that data is thermodynamic consistent.

3.2 Modelling of adsorption equilibrium isotherms

The isotherms plotted in Figure 13 were fitted to the isotherm models shown in Section 2.2. The model fitting of the isotherm models was made by using the Solver tool contained in Microsoft Excel software by minimizing the error of the following equation:

$$\Delta q = \sum_{i=1}^M (q_{cal} - q_{exp}) \quad (25)$$

The most appropriate model will be defined using the best regression coefficient of the fitting R^2 , defined by [36]:

$$R^2 = \frac{(q_{exp} - \overline{q_{cal}})^2}{\sum (q_{exp} - \overline{q_{cal}})^2 - (q_{exp} - q_{cal})^2} \quad (26)$$

3.2.1 Ethylbenzene isotherm model fitting

The adsorption equilibrium isotherms of ethylbenzene on activated carbon by applying different models are compared in Figure 14 with the respective model parameters and regression coefficients resumed in Table 9.

Table 9 Parameters of the different adsorption models for ethylbenzene and regression coefficients.

Model	q_{\max} (mol/kg)	b (1/bar)	$-\Delta H$ (kJ.mol ⁻¹)	K (mol/kg.bar)	n (-)	t (-)	g (-)	R^2 (-)
Langmuir	2.34	143.8	-52.4	-	-	-	-	0.937
Freundlich	-	-	-	3.68	5.12	-	-	0.986
Sips	3.61	37	-59.5	-	2.15	-	-	0.989
Toth	3.71	1055	-50	-	-	0.36	-	0.991
Redlich-Peterson	2.34	141.4	-52	-	-	-	0.99	0.940

* The reference temperature is 398 K.

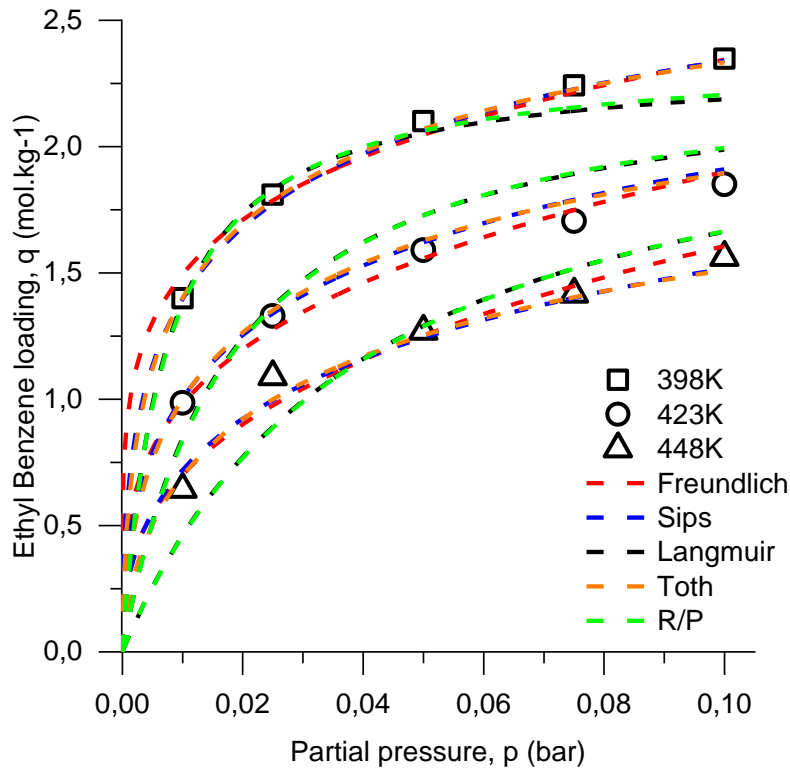


Figure 14 Experimental adsorption equilibrium of ethylbenzene onto Activated carbon Norit RB4 at 398, 423, and 448 K and partial pressure up to 0.1 bar and isotherm models fitting comparison.

Regarding to Figure 14 and the values of the regression coefficients shown in Table 9 it can be concluded that the Toth model is the best for the ethylbenzene adsorption on NORIT RB4 AC. However, the Sips and Freundlich models are also quite representative of the adsorption equilibrium data. It appears that the Langmuir and Redlich-Peterson models are by far the least suitable for describing this system. Langmuir model gives the poorest result probably because the activated carbon is not an energetic homogeneous material. Accordingly, it seems that the adsorption of ethylbenzene on NORIT AC can be considered energetically heterogeneous.

One of the techniques to check the reliability of a model is to illustrate a parity plot with the loading predicted by the models against the loadings of the experimental data [41]. Since the Toth model is the one that best fits the experimental data, the parity diagram is depicted in Figure 15:

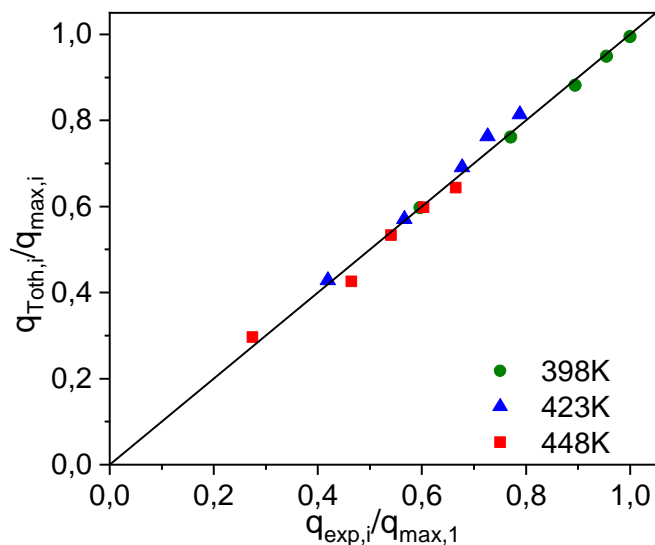


Figure 15 Parity plot of fitted Toth isotherm model for adsorption of ethylbenzene on NORIT RB 4 activated carbon.

Figure 15 proves that at the three experimental temperatures, the Toth model gives a good fit, attesting to its validity to represent the observed experimental values. Also, Table 9 shows the respective heat of adsorption around $50 \text{ kJ}\cdot\text{mol}^{-1}$, a value practically similar for all the isotherms except the one predicted by the Sips model which is around $59.5 \text{ kJ}\cdot\text{mol}^{-1}$. These adsorption heat values are lower than $15 \text{ kcal}\cdot\text{mol}^{-1}$ ($62.76 \text{ kJ}\cdot\text{mol}^{-1}$), meaning that this is a physical adsorption.

3.2.2 n-hexane isotherm mode fitting

The same procedure previously described was applied for the fitting of n-hexane on the NORIT AC. The results are given in Table 10 as well as the comparison of the models to the fitting of the experimental data in Figure 16.

Table 10 Parameters of the different adsorption models for n-hexane.

Model	q_{\max} (mol/kg)	b^* (1/bar)	$-\Delta H$ (kJ.mol ⁻¹)	K^* (mol/kg.bar)	n^* (-)	t^* (-)	g^* (-)	R^2 (-)
Langmuir	1.62	119.6	-54.9	-	-	-	-	0.932
Freundlich	-	-	-	2.65	4.14	-	-	0.988
Sips	2.83	17.5	-59.2	-	2.22	-	-	0.980
Toth	3.96	1995	-52.5	-	-	0.25	-	0.977
Redlich-Peterson	0.51	1867	-58.9	-	-	-	0.78	0.978

* The reference temperature is 398 K.

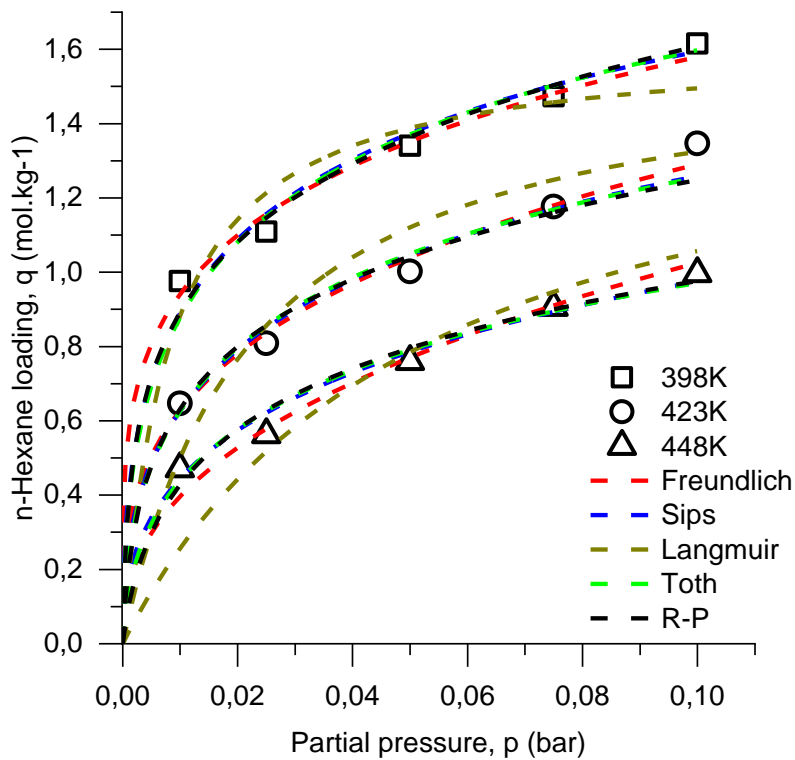


Figure 16 Experimental adsorption equilibrium of n-hexane onto Activated carbon Norit RB4 at 398, 423, and 448 K and partial pressure up to 0.1 bar and isotherm models (a) Toth, (b) Sips, (c) Redlich-Peterson, (d) Langmuir, and (e) Freundlich.

Looking to table 10 and figure 16, we can conclude that for n-hexane the Freundlich model is the most suitable, which is also a heterogeneous model. The parity diagram for the Freundlich isotherm in figure 17, conforms to the accuracy of its description adsorption equilibrium on n-hexane in NORIT AC.

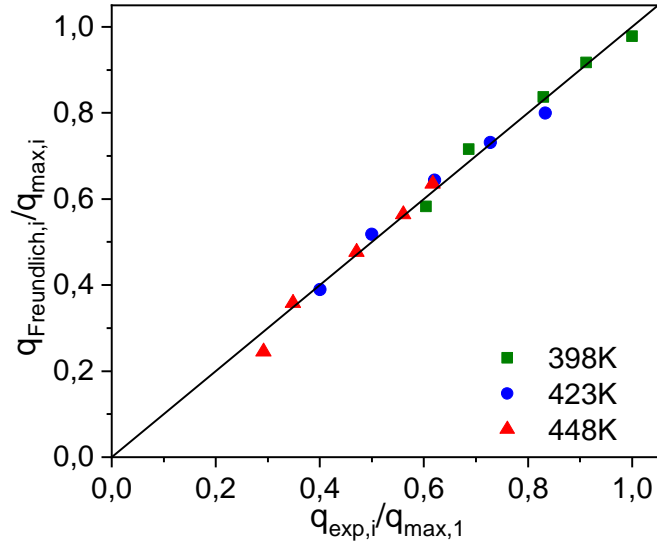


Figure 17 Parity plot of fitted Freundlich isotherm model for adsorption of n-hexane on NORIT RB 4 activated carbon.

Table 10 shows a heat of adsorption is between $52.5 \text{ kJ}\cdot\text{mol}^{-1}$ for the Toth model and $59.2 \text{ kJ}\cdot\text{mol}^{-1}$ for the Sips model. From them values, it can be inferred that this is a physical adsorption

CONCLUSIONS

In this work, a detailed study of the adsorption of ethylbenzene and hexane in commercial activated carbon (Norit RB4) was presented. For that, a chromatographic technique was applied to measure breakthrough curves from where the adsorption equilibrium isotherms were set-up. From the data, sorption uptakes of ethylbenzene up to 2.34 mol.kg^{-1} to 398K and a partial pressure of 0.1 bar were observed, compared to 1.61 mol.kg^{-1} for n-hexane under the same conditions.

The isotherms obtained were then modelled according to Langmuir, Freundlich, Sips, Toth and Redlich-Peterson equations. It was verified that the Toth model is the best for describing the adsorption of ethylbenzene on RB4 reflecting a heterogeneous system, being the Freundlich isotherm model better suited to describe the adsorption of n-hexane, which also suggests that the system is heterogeneous.

In addition, the heat of adsorption of n-hexane is around $52.5 \sim 59.2 \text{ kJ.mol}^{-1}$, and the isosteric heat of ethylbenzene adsorption is around $50 \sim 59.5 \text{ kJ.mol}^{-1}$. The heat of adsorption of these two compounds are quite similar. From these values, it can be deduced that it is a phenomenon of physical adsorption for both compounds.

Finally, it can be concluded that Norit RB4 activated carbon is an efficient adsorbent for removing VOCs such as n-hexane and ethylbenzene from air streams.

In the future, it will be interesting to perform the same breakthrough experiments with mixture of VOCs. Performing a numerical simulation of the fixed bed adsorption runs shown in this work using a proper mathematical model in order to predict the dynamic behavior of these systems fundamental for the design and an adsorption process at a larger scale for the removal of this VOCs from air streams. Also, it will be also interesting to study the adsorption capacity of other aromatic compounds such as xylene or toluene on NORIT RB4 AC.

REFERENCES

- [1] S. S. Anand, B. K. Philip, and H. M. Mehendale, “Volatile Organic Compounds,” in *Encyclopedia of Toxicology: Third Edition*, Third Edit., vol. 4, Elsevier, 2014, pp. 967–970.
- [2] F. Meng, M. Song, Y. Wei, and Y. Wang, “The contribution of oxygen-containing functional groups to the gas-phase adsorption of volatile organic compounds with different polarities onto lignin-derived activated carbon fibers,” *Environ. Sci. Pollut. Res.*, vol. 26, no. 7, pp. 7195–7204, 2019, doi: 10.1007/s11356-019-04190-6.
- [3] Y. Wang, H. Tao, D. Yu, and C. Chang, “Performance assessment of ordered porous electrospun honeycomb fibers for the removal of atmospheric polar volatile organic compounds,” *Nanomaterials*, vol. 8, no. 5, 2018, doi: 10.3390/nano8050350.
- [4] L. Li, Z. Sun, H. Li, and T. C. Keener, “Effects of activated carbon surface properties on the adsorption of volatile organic compounds,” *J. Air Waste Manag. Assoc.*, vol. 62, no. 10, pp. 1196–1202, 2012, doi: 10.1080/10962247.2012.700633.
- [5] L. Zhu, D. Shen, and K. H. Luo, “A critical review on VOCs adsorption by different porous materials: Species, mechanisms and modification methods,” *J. Hazard. Mater.*, vol. 389, no. November 2019, p. 122102, 2020, doi: 10.1016/j.jhazmat.2020.122102.
- [6] M. Ulman and Z. Chilmonczyk, “Volatile organic compounds - Components, sources, determination. A review,” *Chem. Analityczna*, vol. 52, no. 2, pp. 173–200, 2007.
- [7] W. Wei, S. Wang, J. Hao, and S. Cheng, “Projection of anthropogenic volatile organic compounds (VOCs) emissions in China for the period 2010-2020,” *Atmos. Environ.*, vol. 45, no. 38, pp. 6863–6871, 2011, doi: 10.1016/j.atmosenv.2011.01.013.
- [8] C. Yang, G. Miao, Y. Pi, Q. Xia, J. Wu, Z. Li and J. Xiao “Abatement of various types of VOCs by adsorption/catalytic oxidation: A review,” *Chem. Eng. J.*, vol. 370, no. March, pp. 1128–1153, 2019, doi: 10.1016/j.cej.2019.03.232.

- [9] G. Gałezowska, M. Chraniuk, and L. Wolska, “In vitro assays as a tool for determination of VOCs toxic effect on respiratory system: A critical review,” *TrAC - Trends Anal. Chem.*, vol. 77, no. September 2020, pp. 14–22, 2016, doi: 10.1016/j.trac.2015.10.012.
- [10] C. Klett, X. Duten, S. Tieng, S. Touchard, P. Jestin, K. Hassouni and A. Vega-González “Acetaldehyde removal using an atmospheric non-thermal plasma combined with a packed bed: Role of the adsorption process,” *J. Hazard. Mater.*, vol. 279, pp. 356–364, 2014, doi: 10.1016/j.jhazmat.2014.07.014.
- [11] M. S. Kamal, S. A. Razzak, and M. M. Hossain, “Catalytic oxidation of volatile organic compounds (VOCs) - A review,” *Atmos. Environ.*, vol. 140, pp. 117–134, 2016, doi: 10.1016/j.atmosenv.2016.05.031.
- [12] N. Blommaerts, F. Dingenen, V. Middelkoop, J. Salvelkouls, M. Goemans, T. Tytgat, S. W. Verbruggen and S. Lenaerts “Ultrafast screening of commercial sorbent materials for VOC adsorption using real-time FTIR spectroscopy,” *Sep. Purif. Technol.*, vol. 207, no. June 2018, pp. 284–290, 2018, doi: 10.1016/j.seppur.2018.06.062.
- [13] Z. Yang, Y. Lan, Y. Yan, M. Guo, and L. Zhang, “Activation Pathway of C-H and C–C Bonds of Ethane by Pd Atom with CO₂ as a Soft Oxidant,” *ChemistrySelect*, vol. 4, no. 33, pp. 9608–9617, 2019, doi: 10.1002/slct.201902177.
- [14] N. Cheng, D. Jing, C. Zhang, Z. Chan, W. Li, S. Li and Q. Wang “Process-based VOCs source profiles and contributions to ozone formation and carcinogenic risk in a typical chemical synthesis pharmaceutical industry in China,” *Sci. Total Environ.*, vol. 752, p. 141899, 2021, doi: 10.1016/j.scitotenv.2020.141899.
- [15] X. Liang, X. Chen, J. Zhang, T. Shi, X. Sun, L. Fan, L. Wang and D. Ye “Reactivity-based industrial volatile organic compounds emission inventory and its implications for ozone control strategies in China,” *Atmos. Environ.*, vol. 162, no. 2, pp. 115–126, 2017, doi: 10.1016/j.atmosenv.2017.04.036.
- [16] X. Li, L. Zhang, Z. Yang, P. Wang, Y. Yan, and J. Ran, “Adsorption materials for volatile organic compounds (VOCs) and the key factors for VOCs adsorption process: A review,” *Sep. Purif. Technol.*, vol. 235, p. 116213, 2020, doi: 10.1016/j.seppur.2019.116213.

- [17] A. L. Bolden, C. F. Kwiatkowski, and T. Colborn, “New Look at BTEX: Are Ambient Levels a Problem?,” *Environ. Sci. Technol.*, vol. 49, no. 9, pp. 5261–5276, May 2015, doi: 10.1021/es505316f.
- [18] S. R. Clough, “Hexane,” *Encycl. Toxicol. Third Ed.*, vol. 2, pp. 900–904, 2014, doi: 10.1016/B978-0-12-386454-3.00397-3.
- [19] U.S. EPA, “Toxicological review of n-HEXANE,” *Critical reviews in toxicology*, 2005. https://cfpub.epa.gov/ncea/iris/iris_documents/documents/toxreviews/0486tr.pdf.
- [20] International Agency for Research on Cancer, *International Agency for Research on Cancer Iarc Monographs on the Evaluation of Carcinogenic Risks To Humans*, vol. 96. 2002.
- [21] D. Seader and E. J. Henley, *Separation process principles*, vol. 36, no. 09. 1999.
- [22] J. G. Choi, D. D. Do, and H. D. Do, “Surface diffusion of adsorbed molecules in porous media: Monolayer, multilayer, and capillary condensation regimes,” *Ind. Eng. Chem. Res.*, vol. 40, no. 19, pp. 4005–4031, 2001, doi: 10.1021/ie010195z.
- [23] G. Klein and Douglas M. Ruthven, *Principles of adsorption and adsorption processes*, vol. 4, no. 1. 1985.
- [24] B. J. L. Humphrey and G. E. K. Ii, *Separation Process Technology*. New York, 1997.
- [25] M. Domingo-García, F. J. López-Garzón, R. López-Garzón, and C. Moreno-Castilla, “Gas chromatographic determination of adsorption isotherms, spreading pressures, London force interactions and equations of state for n-alkanes on graphite and carbon blacks,” *J. Chromatogr. A*, vol. 324, pp. 19–28, Jan. 1985, doi: 10.1016/S0021-9673(01)81304-2.
- [26] R. C. Bansal and M. Goyal, *Activated Carbon Adsorption*. Boca Raton: CRC Press, 2005.
- [27] Kirk-othmer, *Kirk-othmer Encyclopedia of chemical technology*, 5th Editio. Wiley, 2007.
- [28] G. F. Bennett, *Partition and Adsorption of Organic Contaminants in Environmental Systems*, vol. 98, no. 1–3. 2003.
- [29] D. Saha, N. Miranda, and A. Levchenko, “Liquid and vapor phase adsorption of BTX in lignin derived activated carbon: Equilibrium and kinetics study,” *J. Clean. Prod.*, vol. 182, pp. 372–378, 2018, doi: 10.1016/j.jclepro.2018.02.076.

- [30] Cary T. Chiou, *Partition and Adsorption of Organic Contaminants in Environmental Systems*. New York, 2002.
- [31] M. D. Donohue and G. L. Aranovich, “Classification of Gibbs adsorption isotherms,” *Adv. Colloid Interface Sci.*, vol. 76–77, pp. 137–152, 1998, doi: 10.1016/S0001-8686(98)00044-X.
- [32] C. Megías-Sayago, I. Lara-Ibeas, Q. Wang, S. Le Calvé, and B. Louis, “Volatile organic compounds (VOCs) removal capacity of ZSM-5 zeolite adsorbents for near real-time BTEX detection,” *J. Environ. Chem. Eng.*, vol. 8, no. 2, p. 103724, 2020, doi: 10.1016/j.jece.2020.103724.
- [33] Nashaat N. Nassar, “Iron Oxide Nanoadsorbents for Removal of Various Pollutants from Wastewater: An Overview,” *Appl. Adsorbents Water Pollut. Control*, no. May, pp. 81–118, 2012, doi: 10.2174/978160805269111201010081.
- [34] N. A. Rashidi, S. Yusup, and A. Borhan, “Isotherm and Thermodynamic Analysis of Carbon Dioxide on Activated Carbon,” *Procedia Eng.*, vol. 148, pp. 630–637, 2016, doi: 10.1016/j.proeng.2016.06.527.
- [35] D. D. Do, *Adsorption Analysis: Equilibria and Kinetics*, vol. 2, no. Imperial College Press, 1998.
- [36] K. Y. Foo and B. H. Hameed, “Insights into the modeling of adsorption isotherm systems,” *Chem. Eng. J.*, vol. 156, no. 1, pp. 2–10, 2010, doi: 10.1016/j.cej.2009.09.013.
- [37] N. Tzabar and H. J. M. ter Brake, “Adsorption isotherms and Sips models of nitrogen, methane, ethane, and propane on commercial activated carbons and polyvinylidene chloride,” *Adsorption*, vol. 22, no. 7, pp. 901–914, 2016, doi: 10.1007/s10450-016-9794-9.
- [38] K. Vasanth Kumar, M. M. de Castro, M. Martinez-Escandell, M. Molina-Sabio, J. Silvestre-Albero, and F. Rodriguez-Reinoso, “A continuous site energy distribution function from Redlich-Peterson isotherm for adsorption on heterogeneous surfaces,” *Chem. Phys. Lett.*, vol. 492, no. 1–3, pp. 187–192, 2010, doi: 10.1016/j.cplett.2010.04.044.
- [39] J. Wang and X. Guo, “Adsorption isotherm models: Classification, physical meaning, application and solving method,” *Chemosphere*, vol. 258, p. 127279, 2020, doi:

10.1016/j.chemosphere.2020.127279.

- [40] A. Nuhnen and C. Janiak, “A practical guide to calculate the isosteric heat/enthalpy of adsorption: Via adsorption isotherms in metal-organic frameworks, MOFs,” *Dalt. Trans.*, vol. 49, no. 30, pp. 10295–10307, 2020, doi: 10.1039/d0dt01784a.
- [41] A. Henrique, A. E. Rodrigues, and J. A. C. Silva, “Separation of Hexane Isomers in ZIF-8 by Fixed Bed Adsorption,” *Ind. Eng. Chem. Res.*, vol. 58, no. 1, pp. 378–394, 2019, doi: 10.1021/acs.iecr.8b05126.